

Discrete Equilibrium Sampling with Arbitrary Nonequilibrium Processes

Firas Hamze¹ and Evgeny Andryash¹

¹D-Wave Systems Inc.

June 24, 2021

Abstract

We present a novel framework for performing statistical sampling, expectation estimation, and partition function approximation using *arbitrary* heuristic stochastic processes defined over discrete state spaces. Using a highly parallel construction we call the *sequential constraining process*, we are able to simultaneously generate states with the heuristic process and accurately estimate their probabilities, even when they are far too small to be realistically inferred by direct counting. After showing that both theoretically correct importance sampling and Markov chain Monte Carlo are possible using the sequential constraining process, we integrate it into a methodology called *state space sampling*, which extends the classical ideas of state space search from computer science to the sampling context. The methodology comprises a *dynamic* data structure that constructs a robust Bayesian model of the statistics generated by the heuristic process subject to an accuracy constraint, the *posterior Kullback-Leibler divergence*. Sampling from the dynamic structure will generally yield *partial* states, at which point the heuristic is called recursively to refine the structure at the needed point in the state space until *complete* states, along with their probability estimates, are returned. Importance sampling is thereby enabled. Our experiments on various Ising models strongly suggest that state space sampling enables heuristic state generation with dramatically accurate probability estimates, demonstrated by illustrating the convergence of a simulated annealing process to the Boltzmann distribution with increasing run length. Consequently, heretofore unprecedented direct importance sampling using the *final* (marginal) distribution of a generic stochastic process is allowed, potentially augmenting considerably the range of algorithms at the Monte Carlo practitioner's disposal.

1 Introduction

We consider in this paper the problem of computing expectations of functions with respect to discrete distributions

$$\mathbb{E}_\pi[h(\mathbf{Y})] \tag{1}$$

Without loss of generality, the function π defined over a discrete state space can be assumed to be in *Boltzmann distribution* form

$$\pi(\mathbf{y}) = \frac{e^{-E(\mathbf{y})}}{Z_\pi} \tag{2}$$

where $E(\mathbf{y})$ and $Z_\pi = \sum_{\mathbf{y}} e^{-E(\mathbf{y})}$ are the *energy function* and *partition function* respectively. In this paper, we assume that \mathbf{y} is a vector of m *Ising*-valued variables, i.e

$$\begin{aligned} y_i &\in \{-1, 1\} \\ \mathbf{y} &= y_{1:m} \in \mathbb{S}^m \end{aligned}$$

where $\mathbb{S}^m \triangleq \{-1, 1\}^m$ is the set of all possible Ising configurations on m variables. Modification of the paper's ideas to the cases of Boolean ($\{0, 1\}$) or more general discrete values is straightforward.

The problem defined in Equation (1) arises in a wide range of applications from statistics and machine learning to statistical physics; some examples include computing spin-spin correlations, local magnetizations, and average energies. When performing *Boltzmann machine learning*, access to accurate estimates of these quantities enables *maximum likelihood* parameter estimation [39]; in physics, their behaviour may signal phenomena such as *phase transitions* [8]. Additionally, in several settings such as *approximate counting* [28] and *Bayesian model selection* [4] it is of interest to approximate Z_π .

The task of approximating expectations can, of course, in principle be treated by generating samples from $\pi(\mathbf{y})$ and computing the empirical average of h over those samples. In situations where the problem possesses some simplifying structure such as a low treewidth, this is indeed feasible. In general, drawing such samples for systems with large m is highly nontrivial. A common approach is to use a *Markov Chain Monte Carlo* (MCMC) algorithm instantiating a generally correlated sequence of samples whose distribution converges asymptotically to π ; examples include *Metropolis* [34], *Metropolis-Hastings* [20], and Gibbs (*heat bath*) samplers [14, 16]. The simplest versions of these algorithms are *local* (univariate), but more sophisticated generalizations such *parallel tempering* [15, 26] and *cluster-based* methods [24, 41, 44, 46] have been devised to improve efficiency. When designing such algorithms, special care must be put into ensuring that they yield the correct stationary distribution. Consequently, it is often difficult to engineer a correct algorithm that makes large jumps in the state space and avoids getting trapped in local optima. In addition, approximating Z_π using MCMC is not automatically obvious.

An alternative to MCMC is *importance sampling*, where one generates samples according to some *trial* (or *proposal*) distribution and appropriately weights their contribution in the estimator to ensure that a statistical average with respect to π is obtained. This method can suffer from terrible

inaccuracy in high-dimensional problems. The main issue is that it becomes exceedingly difficult to design a trial distribution that is simultaneously *tractable*, i.e. allowing efficient sampling and, for the purpose of reweighting, evaluation, and possesses sufficient *overlap* with the statistically-dominant regions of the state space under π . To illustrate two extremes, using a uniform trial distribution certainly satisfies the tractability requirement, but will typically require a completely unrealistic number of samples to yield useful estimates for most interesting problems; on the other hand, one can conceivably design an elaborate, randomized heuristic process which covers the important areas of π quite well, but computing the probabilities of states yielded by such a process may be infeasible. As a concrete example of the latter case, one may be interested in probing the statistics of the global energy minima, or *ground states*, of E . These states occur with uniform probability under π at zero temperature. The question of how to perform estimation when given access to a heuristic that generates ground states with unknown and generally nonuniform probabilities is a subset of the problems tackled by the approach taken in this paper.

The class of algorithms known as *sequential Monte Carlo* (SMC) (or *population annealing*) methods [12, 25, 27, 33, 43] are in some sense a synthesis of importance sampling and MCMC. In general, applying a finite number of MCMC moves will yield a distribution that is *out of equilibrium*, in other words, has not yet converged to π . Were one able to evaluate this nonequilibrium probability, an estimator using reweighted samples could compensate for the finite stopping-time bias incurred by naïvely using the raw empirical average. Computing the nonequilibrium distribution is generally out of the question; SMC methods circumvent this difficulty by *augmenting* the state space under consideration to a *joint, growing* one. For example suppose we could tractably sample from distribution $\pi_0(\mathbf{y}_0)$ and generate updated state \mathbf{y}_1 according to an MCMC kernel T converging to $\pi(\mathbf{y}_1)$; of course, the variables $(\mathbf{Y}_0, \mathbf{Y}_1)$ will be jointly distributed according to $\pi_0(\mathbf{y}_0)T(\mathbf{y}_1|\mathbf{y}_0)$. If we suitably define an *augmented* target distribution to be $\pi(\mathbf{y}_1)L(\mathbf{y}_0|\mathbf{y}_1)$, where $L(\mathbf{y}_0|\mathbf{y}_1)$ is a conditional distribution which can in general be chosen with great flexibility, we could use the importance-weighted samples *over the joint state space* to approximate the expectation of $h(\mathbf{y}_1)$ with respect to π . The idea can be extended to a *sequence* of target distributions (π_n) , typically obtained by *annealing* a temperature parameter scaling the energy such that the final distribution in the sequence is the target π . The variance of estimator grows with the length of the sequence, and hence variance reduction techniques, such as the (asymptotically) unbiased strategy of *resampling* (or *particle interaction*) are often applied. A particularly desirable attribute of SMC methods is that they enable estimation of the partition function Z_π if that of the initial distribution $\pi_0(\mathbf{y})$ is known.

SMC methods have been a considerable advance in Monte Carlo simulation, but they still impose certain restrictions on the practitioner. One particularly unappealing aspect of a commonly-applied variant of SMC is that, due to the usage of a growing state space, a sequence of distributions with considerable overlap is required even if the proposal kernel T happens to yield *perfect* samples from the distribution it targets. Furthermore, while it is possible in principle to use a more generic move process than an MCMC operator, designing an appropriate joint distribution via $L(\mathbf{y}_0|\mathbf{y}_1)$ then becomes nontrivial. For example, a tempting possibility is to simply choose $L(\mathbf{y}_0|\mathbf{y}_1) = \pi(\mathbf{y}_0)$,

yielding a simple-looking expression for the importance weights. Unfortunately, a serious issue is that the proposal can typically only be evaluated exactly for *local* moves. This in turn implies that the overlap between π and $T(\mathbf{x}_1|\mathbf{x}_0)$ can be negligible, leading to tremendous variance. The issue would be mitigated one could somehow instantiate a proposal that achieved good global coverage of π , but in that case its evaluation becomes impossible. Indeed it is precisely this central issue that motivates the present work and its ramifications.

Our approach departs from the SMC methodology of importance sampling on a growing state space and reverts to directly using the distribution of the final state of an arbitrary heuristic process. The methodology could considerably expand the repertoire of tools at researchers’ disposal with which to perform statistical sampling. For example, one may now employ, in place of commonly-used MCMC methods relying on single variable updates, randomized combinatoric methods (such as *primal-dual algorithms* and *linear programming with rounding*) whose distributions are exceedingly difficult to characterize, but which nonetheless may be excellent trial processes with which to sample from a target distribution. Alternatively, well-known MCMC algorithms may be modified in such a way as to improve their mobility in the state space, despite the generally crucial property of *detailed balance* being consequently broken; for regular MCMC methods, it provides a compelling diagnostic of convergence. Finally, physical sampling devices with real-world imperfections causing unknown changes to their distributions may be brought to bear [29,47]. As mentioned, our focus in this work is on distributions over discrete state spaces, but the general ideas are certainly transferable to the continuum in principle.

In Section 3, we introduce the *Sequential Constraining Process*, the central workhorse of our algorithms. Given a stochastic sampling heuristic as a “black box”, this process instantiates states along with relatively accurate estimates of their probabilities. It does so by constructing, using a sample *population* from the heuristic, a *statistical model* subject to an accuracy criterion. In general, this model will not be able to represent the full state space for a realistically-sized population. Nonetheless, when a sample is drawn from the model corresponding to an incomplete state, the heuristic can be used *recursively* to construct another accuracy-respecting model with the incomplete state as a *constraining condition*. In this manner, full states and probabilities are generated by stochastically *querying* the proposal. Like most population-based methods, the sequential constraining process is a highly parallelisable algorithm, and can hence straightforwardly leverage the ubiquitous computing power available at the time of this paper’s writing. The issue of parameter estimation, i.e. construction of the modelling distributions, is a crucial one and is discussed in Section 3.3. We opt for a *robust Bayesian* approach to estimating the heuristic distributions, with the *posterior Kullback-Leibler divergence* as the loss function quantifying estimator accuracy. Rao-Blackwellisation as a means of *variance reduction* is presented in 3.3.3.

In Section 4, we show the crucial fact that the sequential constraining process allows *both* importance sampling and MCMC to be performed. This is of particular interest as our algorithms are *theoretically correct* but employ as proposals *approximations* to a complicated distribution; it is *not* generally true that valid Monte Carlo results when such approximations are made.

Section 5 coalesces the introductory ideas of the first half of the paper into a practical importance

sampling algorithm we call *state space sampling*. The name is motivated by the class of algorithms used in artificial intelligence known as *state space search*, a generalization of which it can be seen¹. State space sampling is a process by which discrete states are drawn by sampling from a *dynamical* statistical model of an unknown proposal heuristic, estimated from populations generated using the constraining process. For binary state spaces, the dynamical model is naturally represented as a *binary tree* whose nodes correspond to partial states within the state space. The sampling procedure can be seen as a stochastic *exploration* of this binary tree; when a node is reached corresponding to an incomplete state, the model tree is extended from that point by invoking the proposal process with the partial state constraint for a fresh population, growing a new model, and resuming the sampling. Ideally, the model constructed would be retained (or *cached*) as long as samples are being drawn, but just as is done in the search context, a bound on the tree size must be imposed to respect practical memory constraints. We propose implementing this in a manner such that regions of the model that have lower probability of being used have higher *priority* for being discarded. A simple example illustrating the main features of state space sampling is presented in Section 5.2.

Section 6 discusses experimental results obtained by applying state space sampling to several types of Ising model using short-run simulated annealing processes as the stochastic heuristic. While the point of devising the methodology in this paper was to allow for the use of more general heuristics, we nonetheless selected simulated annealing in this preliminary illustration because its behaviour is relatively well-understood. More specifically, if we claim that our methodology allows for accurate estimation of distributions derived from arbitrary heuristics, which would then in turn enable reliable importance sampling should the heuristic distribution be a good match to the target, then applying simulated annealing should unambiguously show convergence of the states' estimated probabilities to the final target distribution π as the run length is increased. The results presented in Section 6 indeed provide such confirmation, showing convergence of the ensemble distribution to π in a fairly direct manner. Throughout the paper, we strive to maximize computational efficiency, either generically or, using problem-dependent features as discussed in Appendix 9.1.

Our analysis and results show state space sampling, and the general methodology presented in this paper, to be a potentially powerful framework that takes advantage of copious contemporary computing power and considerably enlarges the scope of algorithms that can be used to simulate complex systems.

2 Notational Preliminaries

Following common convention, random variables appear in upper case, with their particular values in lower case. Variables appearing in bold are vector-valued; e.g. $\mathbf{y} \in \mathbb{R}^m$. When appearing with subscripts, bold symbols refer to elements of a sequence of vector-valued variables; e.g. $\mathbf{y}_n \in \mathbb{R}^m$. Plain symbols can refer to either scalar or multivariate values depending on the form of their

¹Though correctness of an MCMC algorithm using approximations derived from the heuristic process is shown in principle, practical exploration of this is left to future work.

subscripts. For example y_n refers to the n^{th} element of \mathbf{y} , but $y_{1:n}$ refers to first n elements of \mathbf{y} (hence $y_{1:m} = \mathbf{y}$). More generally, y_I specifies the variables in \mathbf{y} indexed by subset $I \subseteq \{1, \dots, m\}$, e.g. if $I = \{1, 3, 10\}$, then y_I is short for $\{y_1, y_3, y_{10}\}$. On the other hand, $U_{n,I}$ denotes the variates indexed by I in the n^{th} vector-valued \mathbf{U}_n appearing in a sequence. Finally, superscripts in parentheses refer to members of a set of random variables instantiated from some distribution. For example to denote drawing N samples from distribution f , we write $\mathbf{Y}^{(j)} \sim f$ for $j = 1, \dots, N$. Illustrating some of these conventions, the conditional distribution of variable \mathbf{X} given the first n elements of $\mathbf{y}^{(j)}$, the *observed* value of the j^{th} sample, would be written as $f(\mathbf{x}|y_{1:n}^{(j)})$.

3 The Sequential Constraining Process

3.1 Sampling with Nonequilibrium Distributions

Suppose we have available a stochastic procedure, referred to as the *proposal process* \mathcal{P} , generating samples from some discrete probability distribution. Particular simulation-based examples are Markov Chain Monte Carlo (MCMC) algorithms run for a finite number of iterations, where consequently, the asymptotic distribution is generally not reached, non-Markovian *stochastic local search* (SLS) algorithms [23] that may either start from a completely uniform distribution or, as in the case of *iterated* local search, generate configurations conditioned on the current state, and methods that allow for interactions among members of a population such as *genetic* or *evolutionary* algorithms [17, 22]. Alternatively, \mathcal{P} can correspond to deriving configurations from a physical system such as one designed to implement a thermal or quantum annealing algorithm.

With exceptions such as MCMC, little can be theoretically said of any statistical or convergence properties of these processes. Thus, while they may be useful as randomized heuristics to generate low-energy (or “low-cost”) configurations of a system, in raw form they are unsuitable for performing correct stochastic simulation of a specified probability distribution π with respect to that system. In the following, we discuss this issue in such a way as to motivate the contributions of this paper.

Let $f(\mathbf{y}|\mathbf{x})$ be the probability of sampling $\mathbf{y} \in \mathbb{S}^m$ by running \mathcal{P} to completion from current state $\mathbf{x} \in \mathbb{S}^m$. If \mathcal{P} corresponded to some “perturbative” process such as a sequence of MCMC or SLS moves, then $f(\mathbf{y}|\mathbf{x})$ is the *marginal distribution* of the state at the final time step of \mathcal{P} . For certain kinds of \mathcal{P} , such as finite-length MCMC from a random initial state, $f(\mathbf{y}|\mathbf{x}) = f(\mathbf{y})$, and in such cases we will omit the dependence in the notation. We emphasize to readers familiar with SMC not to confuse $f(\mathbf{y}|\mathbf{x})$ with the *joint* probability of a sample path resulting from a sequence of proposal moves.

Given that we can sample from $f(\cdot)$, two well-known methodologies that would *in principle* allow for estimation of expectations are *Importance Sampling* (IS) and the *Metropolis-Hastings* (MH) MCMC algorithm. In the case $f(\mathbf{y}|\mathbf{x}) = f(\mathbf{y})$, we could have

$$\mathbb{E}_\pi[h(\mathbf{Y})] = \mathbb{E}_f[w(\mathbf{Y})h(\mathbf{Y})] \tag{3}$$

where the *importance weights* are given by

$$w(\mathbf{y}) \triangleq \frac{\pi(\mathbf{y})}{f(\mathbf{y})}$$

For a correlated proposal, arising for example from applying an iterated local search idea, the standard MH algorithm can be used to asymptotically sample from π , which would in turn allow estimation. The point \mathbf{y} generated according to $f(\cdot|\mathbf{x})$ would be accepted with probability

$$\alpha(\mathbf{x}, \mathbf{y}) \triangleq \min \left[1, \frac{\pi(\mathbf{y})f(\mathbf{x}|\mathbf{y})}{\pi(\mathbf{x})f(\mathbf{y}|\mathbf{x})} \right] \quad (4)$$

When f itself corresponds to running a MCMC algorithm for some number of time steps, this can be viewed as an "outer" MCMC loop.

Unfortunately, these two approaches are utterly impractical for many interesting choices of proposal distribution. The difficulty lies in the requirement to evaluate $f(\mathbf{y})$ for IS and of the *forward* and *reverse* proposal probabilities, $f(\mathbf{y}|\mathbf{x})$ and $f(\mathbf{x}|\mathbf{y})$ respectively, to perform MH sampling. Consider the simple case that f was instantiated by a sequence of $k + 1$ Markov operations $\{T_k\}$ (such as local-variable simulated annealing) so that

$$f(\mathbf{y}|\mathbf{x}) = \sum_{\mathbf{s}_1 \dots \mathbf{s}_k} T_{k+1}(\mathbf{y}|\mathbf{s}_k) \dots T_1(\mathbf{s}_1|\mathbf{x})$$

Even if the Markovian property were exploited, computing the summations would require exponential (in m) time; the task is certainly no simpler for generic f . When the proposal arises from a physical system exhibiting unknown or intractable complexity, for example a manufactured implementation [29] of quantum annealing [30], precise characterization of f may be all but impossible.

One may ask if there exists a sensible strategy to approximate $f(\mathbf{y})$ at a sampled point \mathbf{y} . A naïve option is to draw a set of N samples and to approximate $f(\mathbf{y})$ by its histogram

$$f(\mathbf{y}) \approx \frac{1}{N} \sum_i \mathbb{1}_{\mathbf{y}}[\mathbf{y}^{(j)}]$$

where $\mathbb{1}_{\mathbf{y}}[\cdot]$ is the indicator function. In high dimensions, this is generally a flawed approach. Indeed, suppose that a hypothetical "oracle" generated configurations distributed exactly according to target distribution π , but that one was unaware of this and tried to perform importance sampling relative to the histogram estimator instead. For computationally reasonable values of N , and large, non-trivial systems, each sampled point will tend to occur only a few times in the population, and thus its proposal probability will simply evaluate to $\frac{1}{N}$, leading to an importance weight proportional to π ; specifically, in a population where each state is hit a single time, the weights are $w(\mathbf{y}^{(j)}) = \pi(\mathbf{y}^{(j)}) / \sum_j \pi(\mathbf{y}^{(j)})$. This will result in a highly skewed estimator as the correct weights in this scenario are unity by construction. In essence, the *effective* constructed proposal fails to cover the

target; only for extremely large N will the histogram estimates eventually approach their correct values and this effect be mitigated. The main point is that merely being able to sample from a good proposal is not sufficient; one must also be able to accurately *evaluate* it.

Consider now the unknown proposal factorized into its univariate conditionals

$$f(\mathbf{y}|\mathbf{x}) = f_1(y_1|\mathbf{x})f_2(y_2|y_1, \mathbf{x}) \dots f_m(y_m|y_{1:m-1}, \mathbf{x}) \quad (5)$$

While the variables $y_{1:m}$ refer to the *final* configurations jointly yielded by the process, it is instructive to consider the task of generating them in a sequential manner by successively sampling from the conditionals. Suppose we conceptually decomposed the problem of generating the samples from f into m steps. At step 1, we sample a state \mathbf{U} from the joint $f(\mathbf{u}|\mathbf{x})$ and set $Y_1 \leftarrow u_1$. Clearly, Y_1 is then a sample from $f_1(y_1|\mathbf{x})$. At step 2, we sample another state \mathbf{U} from the joint $f(\mathbf{u}|\mathbf{x})$. If $u_1 = y_1$ in this sample, then we set $Y_2 \leftarrow u_2$ and continue; otherwise, we continue to generate additional samples $\{\mathbf{U}\}$ from the joint until $u_1 = y_1$. It can readily be shown that this procedure, a simple form of *rejection sampling*, will yield a sample from the conditional $f_2(y_2|y_1, \mathbf{x})$. In general, at step n , given values $y_{1:n-1}$, one can in principle sample Y_n from the conditional $f_n(y_n|y_{1:n-1}, \mathbf{x})$ by repeatedly drawing $\{\mathbf{U}\} \sim f(\mathbf{u}|\mathbf{x})$ until the condition $u_{1:n-1} = y_{1:n-1}$ is met, setting $Y_n \leftarrow u_n$ for the sample \mathbf{U} that meets the condition. Performing this operation sequentially for $n = (1, \dots, m)$, the random variable $\mathbf{Y} \triangleq Y_{1:m}$ is therefore distributed as $f(\mathbf{y}|\mathbf{x})$.

At first sight, this seems like a puzzling and contrived way of sampling from $f(\mathbf{y}|\mathbf{x})$; indeed, any sample used in the procedure is assumed to come from that very distribution! The reason for its potential interest is that, were one able to carry it out, it would enable *estimation* of the conditional components $\{f_n(y_n|y_{1:n-1}, \mathbf{x})\}$ and thus of the full joint $f(y_{1:m}|\mathbf{x})$.

Estimation of the first few conditionals in (5) indeed turns out to be realistic. For example, unlike attempting to estimate $f(\mathbf{y}|\mathbf{x})$ over the full state space \mathbb{S}^m , it is quite reasonable to approximate the scalar, binary function $f_1(y_1|\mathbf{x})$ using either a histogram or other methods to be discussed later. It is possible in principle to estimate $f_n(y_n|y_{1:n-1}, \mathbf{x})$ using the same idea, but unfortunately, the probability of generating a state from the joint matching a particular signature $y_{1:n-1}$ decreases exponentially with n , and so unsurprisingly, the dimensionality issues recur.

There is no obvious way around this issue if one were to insist on sampling from $f(\mathbf{y}|\mathbf{x})$, but there is a potential solution if one were willing to instantiate another proposal *derived* from \mathcal{P} whose behaviour can be expected to be *similar* to that of \mathcal{P} . In the next section, we discuss this idea, which is one of the main building blocks of our algorithms. Crucial practical matters will be discussed in later sections.

3.2 Sequential Constraining Process Introduced

We begin by illustrating how to recursively invoke the heuristic in such a way as to implicitly define a distribution which can both be sampled from and evaluated. This in some sense sidesteps the rejection sampling difficulties discussed in the last section. Consider first running the proposal

process with respect to a *constrained subsystem* of the overall distribution. More precisely, the heuristic is modified so that some subset of the variables is ensured of having specific values $\{y_i\}$. For reasons that will become clear soon, we refer to the variates generated by such a process as \mathbf{U} in distinction to \mathbf{Y} . An example of a proposal targeting a constrained subsystem is using a SLS or MCMC heuristic, holding constant from the initial conditions the values of variables U_I to y_I for some subset I of the variable indices, and running the process to completion on the remaining variables. Alternatively, it may be preferable to *gradually* apply a local bias (or “field”) whose magnitude increases over the course of the simulation such that the final values of U_I are constrained to being y_I .

The joint proposal distribution with a given set of constraints imposed (either by *hard clamping* from initial conditions or by increasing their effect over the course of \mathcal{P}) is defined for $n \geq 2$ to be

$$q_n(\mathbf{u}|y_{1:n-1}, \mathbf{x}) = \left[\prod_{k=1}^{n-1} \delta_{y_k}(u_k) \right] q_n(u_{n:m}|u_{1:n-1}, y_{1:n-1}, \mathbf{x}) \quad (6)$$

Equation 6 makes explicit that in a simulation from q_n , variables $U_{1:n-1}$ will have prescribed values $y_{1:n-1}$ with probability one. The conditional on the RHS of 6 is only defined for $u_{1:n-1} = y_{1:n-1}$ as all \mathbf{u} without this property have a joint probability of zero. We can thus shorten the notation and use $q_n(u_{n:m}|y_{1:n-1}, \mathbf{x})$ to refer implicitly to this conditional; likewise $q_n(u_n|y_{1:n-1}, \mathbf{x})$ refers to the conditional of variable u_n when constraints $y_{1:n-1}$ are imposed. Finally, the case of $n = 1$ is defined to be such that no constraint is imposed. In other words, $q_1(\mathbf{u}|\mathbf{x}) = f(\mathbf{u}|\mathbf{x})$, which is simply the original proposal. The distinction between the conditionals of the original process

$$\{f_n(y_n|y_{1:n-1}, \mathbf{x})\}$$

and those of the constrained process

$$\{q_n(u_n|y_{1:n-1}, \mathbf{x})\}$$

should be borne in mind; except at $n = 1$, they are generally not the same. The $\{f_n\}$ are simply those of the proposal when \mathcal{P} is run without any of the aforementioned constraining mechanisms and random variables $Y_{1:n-1}$ *happened to have* values $y_{1:n-1}$. In the constrained case, we are forcefully changing the “dynamics” of \mathcal{P} such that the constraints are met. In many situations, the two families of conditionals can be expected to be close: for example if \mathcal{P} corresponds to an MCMC process with invariant distribution π , then both $f_n(y_n|y_{1:n-1}, \mathbf{x})$ and $q_n(y_n|y_{1:n-1}, \mathbf{x}) \Rightarrow \pi(y_n|y_{1:n-1})$ as the process length increases.

Simulating constrained subsystems suggests an algorithm to sample from *and approximate* a surrogate to f . We now describe a rudimentary version, which we call the *Sequential Constraining Process* (SCP.) First, note that once constraint $y_{1:n-1}$ is imposed, we are free in principle to generate as much data as desired from $q_n(u_{n:m}|y_{1:n-1}, \mathbf{x})$ by repeatedly calling the constrained heuristic. In particular, a population of sufficient size can be drawn so as to reliably estimate the univariate

conditional $q_n(u_n|y_{1:n-1}, \mathbf{x})$. This is in distinction to sampling from $f_n(y_n|y_{1:n-1}, \mathbf{x})$, which would, as discussed, require a generally intractable rejection sampling procedure. In this paper, to estimate $q_n(u_n|y_{1:n-1}, \mathbf{x})$ we shall consider only *consistent* statistical estimators, i.e. those converging in probability to the true value of the estimand with increasing population size N . For the problems of present interest, the univariate conditional estimation problem is simply that of approximating a binomial success parameter given N binary observations. Examples of consistent estimators for this parameter are the MLE histogram and its Bayesian analogues under a prior distribution over the parameter values. Estimation will be discussed in detail in Section 3.3, but for now, given a population $\{\mathbf{u}_n^{(j)}\}$ of size N from $q_n(u_{n:m}|y_{1:n-1}, \mathbf{x})$, we approximate the distribution of the n^{th} variable with the consistent estimator:

$$\hat{q}_n(y_n|\{\mathbf{u}_n^{(j)}\}, y_{1:n-1}, \mathbf{x}) \approx q_n(y_n|y_{1:n-1}, \mathbf{x})$$

After constructing \hat{q}_n , we trivially sample a value y_n from the estimator and repeat the process for the next variable. Following a suitable initialization, this methodology defines the SCP; it is summarized in Algorithm 1. A complete binary state \mathbf{y} is generated in this manner, and importantly, *so is an approximation to its joint probability under the SCP*. More specifically, we have the joint approximation

$$\hat{q}(\mathbf{y}|\mathbf{x}) = \prod_{n=1}^m \hat{q}_n(y_n|\{\mathbf{u}_n^{(j)}\}, y_{1:n-1}, \mathbf{x}) \quad (7)$$

Figure 1 visually shows the statistical structure of the procedure for the case of sampling three binary variables. We now see why it was necessary to distinguish between variables \mathbf{Y} and \mathbf{U} . The latter, corresponding to variates generated by simulating constrained subsystems, are used to construct estimators, but are ultimately not the states returned by the algorithm. The final “usable” states, \mathbf{Y} , are sampled from the estimators

We remark that there is considerable algorithmic flexibility here. The heuristics used in different clamping stages need not have the same parameters. Suppose, for instance, that a simulated annealing-type process is used as the heuristic. As variables get sequentially clamped, the state spaces effectively simulated over are of course decreasing in size. One can accordingly use increasingly fast annealing schedules for each process in the sequence. It is generally the case that heuristics tend to more effectively probe the low-energy structure of a problem landscape as the number of problem variables is reduced.

The flexibility inherent to SCP is in fact more general than allowing for the heuristic parameters to be tailored to the relative order in the sequence: the formulation allows us to altogether move away from reliance on a *single* heuristic process for sampling. The heuristics themselves invoked in the sequence are allowed to be completely different, and may even depend on the particular state of the system. A general rule is that if one can derive a favorable heuristic for a system of a certain size, then one can also find *some* heuristic for a constrained subsystem; simulating small systems is typically no harder than simulating larger ones. Hence, if a more efficient heuristic is known for simulating a subsystem than for simulating the full system, a SCP can be defined that

applies the appropriate heuristic to the system under consideration. The state \mathbf{y} can in that case be interpreted as arising from a “compound” heuristic process. As an example of this sort of heuristic mixing, suppose that at some point in the sequence which began using a local search proposal, the set of variables has fractured into small enough independent sets that *exact* samples can be feasibly generated. The exact sampling algorithm can then serve as the “heuristic” called recursively at that point, and the values of the corresponding (exact) conditional probabilities can be used in place of an approximately determined \hat{q}_n . In this introductory paper we focus on presenting and validating the basic ideas, leaving in-depth experimentation with large number of plausible heuristics to a later analysis. Section 7 discusses some additional heuristic possibilities.

In summary, the advantage of the SCP methodology is that samples from a favorable heuristic proposal (or class of proposals) can be faithfully generated and their generation probabilities accurately approximated. As discussed in Section 4, this enables the heuristics to be used for Monte Carlo estimation.

Algorithm 1 Basic Sequential Constraining Process (SCP)

Initialize

Draw N samples $\{\mathbf{U}_1^{(j)}\} \sim q(\mathbf{u}|\mathbf{x})$
Construct $\hat{q}_1(y_1|\{\mathbf{u}_1^{(j)}\}, \mathbf{x})$ (see Section 3.3)
Sample $Y_1 \sim \hat{q}_1(y_1|\{\mathbf{u}_1^{(j)}\}, \mathbf{x})$

for $n = 2, \dots, m$ **do**

Draw N samples $\{\mathbf{U}_n^{(j)}\} \sim q_n(u_{n:m}|y_{1:n-1}, \mathbf{x})$
Construct $\hat{q}_n(y_n|\{\mathbf{u}_n^{(j)}\}, y_{1:n-1}, \mathbf{x})$ (see Section 3.3)
Sample $Y_n \sim \hat{q}_n(y_n|\{\mathbf{u}_n^{(j)}\}, y_{1:n-1}, \mathbf{x})$

end for

We presently discuss a few aspects of the SCP. First, we remark that the members of the populations $\{\mathbf{U}_n^{(j)}\}$ generated by the constrained runs of \mathcal{P} are *not required to be statistically independent*. This is of particular importance if considering the use of heuristics that involve *interaction* among the samples. Practically significant instances of such interaction are *stochastic resampling* [12,25,33] and *genetic crossover* [17,22].

The computational inefficiency of the presented variant of the SCP should be apparent. In its described form, it requires sampling a population of size N for *each discrete variable* in the target distribution to compute the estimators $\{\hat{q}_n\}$ for the generation of a *single sample* \mathbf{y} . Given that generating each sample for estimator construction requires running a heuristic, even if the trivially parallel nature of the task were exploited, this seems like a wasteful undertaking. Some speedup can be straightforwardly achieved by estimating conditionals of *groups* (or *blocks*) of variables; instead of estimating binomial success probabilities, the task becomes that of *multinomial* estimation. But this approach needs to be applied with caution: if the binary state spaces corresponding to the

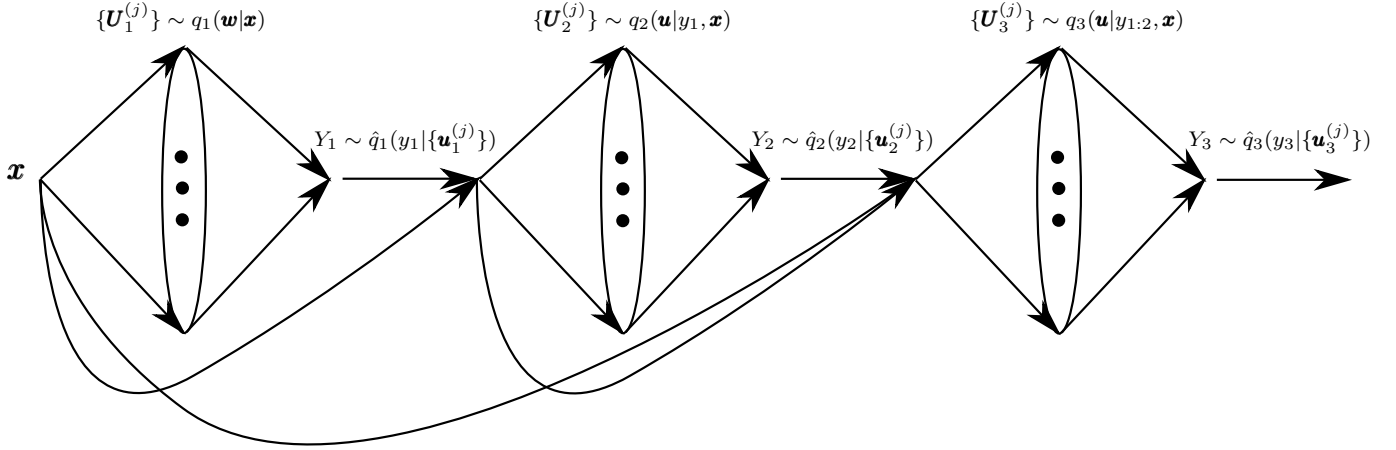


Figure 1: Illustration of the sequence of statistical operations implementing a simple variant of the *Sequential Constraining Process* (SCP) to generate samples using an arbitrary stochastic process. At each stage, a possibly dependent population of samples $\{\mathbf{u}_n^{(j)}\}$ is generated by running the process with variables $y_{1:n-1}$ clamped to their preceding values (none for the initial stage.) A consistent estimator $\hat{q}_n(y_n|\{\mathbf{u}_n^{(j)}\}, y_{1:n-1})$ is then constructed, and variable y_n is sampled from this estimator. The result is a binary state \mathbf{y} and an approximate value of its probability $\hat{q}(\mathbf{y}|\mathbf{x}) = \prod_{n=1}^3 \hat{q}_n(y_n|\dots)$ under the SCP.

block variables are too large relative to the population size N , the resulting estimators \hat{q}_n (where n is now a block index rather than a single variable index) will degrade rapidly, even if perfect equilibrium samples were generated by the proposal. The compromise we ultimately use, leveraging ideas of Bayesian robustness, is to construct a discrete state space of approximately maximum size, corresponding to a *partition* of the set of binary outcomes realizable by a block of variables, such that a maximum tolerable statistical risk is never exceeded. Algorithmically, we strive to build a maximum binary tree subject to a statistical loss constraint. In Section 5, we will present a novel, adaptive methodology for discrete variable generation using the notion of sequential constrained sampling that alleviates some of the computational shortcomings using our robust Bayesian tree construction and incorporating some ideas of *state space search* from classical artificial intelligence. We reassure the reader that an example clearly illustrating the combination of these ideas will be presented in 5.2, and apologize for the technical labyrinth that intercedes.

In Section 4, we will show that one can in principle perform correct Monte Carlo estimation with the naïve variant of the SCP presented here using both importance sampling and MCMC. In the next section, however, we take a diversion into the important subject of construction of the estimators $\{\hat{q}_n\}$ used in the SCP.

3.3 Estimators of q_n in SCP

To ease the notation, we drop the dependence of the heuristic on \mathbf{x} in this section, as we do when discussing importance sampling in Section 4.1, where typically the heuristic distribution is not

dependent on the initial state. The dependence will recur when we present SCP-based MCMC in Section 4.2.

3.3.1 Preliminaries

Suppose we possess a collection of N samples $\{\mathbf{u}^{(j)}\}$. Let I be a subset of the variable indices, i.e. $I \subseteq \{1, \dots, m\}$, and y_I refer to a binary state on the corresponding variables. We define the counting function

$$\#[y_I; \{\mathbf{u}^{(j)}\}] \triangleq \sum_{j=1}^N \mathbb{1}_{y_I}[\mathbf{u}_I^{(j)}] \quad (8)$$

which simply indicates the number of times the binary string y_I occurs in the samples $\{\mathbf{u}^{(j)}\}$.

Consider the case in which we seek to approximate the univariate function $q_n(y_n|y_{1:n-1})$. A possible choice is the *histogram* or *maximum likelihood estimator* (MLE)

$$\hat{q}_n(y_n|\{\mathbf{u}_n^{(j)}\}, y_{1:n-1}) = \frac{\#[y_n; \{\mathbf{u}_n^{(j)}\}]}{N} \quad (9)$$

An undesirable property of the MLE in the present context is that it assigns zero success probability when the observed success count is zero. This can cause serious theoretical and practical issues for our algorithms.

Bayesian estimators, which obtain from minimizing the *Bayes risk* over a suitable *loss function* (often the *squared loss*) under a hypothesized *prior*, are appealing because for many prior distributions, they never evaluate to zero for a finite number of observations. It is not our intention to delve into the details of Bayesian analysis here (see e.g. [3, 4]) but we recall a few relevant facts. When performing inference on the success probability of binomially-distributed data, it is common to assume that the parameter follows a *beta distribution* with two non-negative *hyperparameters*. The *posterior* distribution of the success probability will then also be beta. In our situation, let $\alpha(y_n)$ refer to the prior parameter corresponding to outcome $y_n \in \{+, -\}$. The estimator that minimizes the posterior expected *squared loss* is then

$$\hat{q}_n(y_n|\{\mathbf{u}_n^{(j)}\}, y_{1:n-1}) = \frac{\#[y_n; \{\mathbf{u}_n^{(j)}\}] + \alpha(y_n)}{N + \alpha(+)+\alpha(-)} \quad (10)$$

Many other loss functions are possible; in this work, we use the *Kullback-Leibler loss* as discussed and justified in Section 3.3.2. The Bayes estimator with respect to that loss happens to be the same as that under the squared loss.

It is common to set $\alpha(+)=\alpha(-)$ in the absence of information suggesting a preference towards either outcome; within this family of *symmetric* (or “non-informative”) beta distributions are the *Laplace* prior ($\alpha(+)=\alpha(-)=1$) corresponding to a uniform distribution on the success parameter, and *Jeffreys’* prior ($\alpha(+)=\alpha(-)=0.5$), which leaves the posterior distribution invariant under a

monotone transformation of the success parameter and is hence termed the *objective* prior for the binomial parameter.

The Bayesian binomial analysis is straightforwardly generalized to the multinomial case; the K -category extension of the beta distribution is the *Dirichlet distribution* with nonnegative hyperparameter vector $\boldsymbol{\alpha} \in \mathbb{R}^K$. When the set of outcomes, defined as \mathcal{Y}_I , consists of all $2^{|I|}$ possible binary configurations on variables I , let $\alpha(y_I)$ be the prior hyperparameter corresponding to particular string y_I . The analogous Bayes estimator to (10) for the probability $q_n(y_I|\{\mathbf{u}_n^{(j)}\}, y_{1:n-1})$ is

$$\hat{q}_n(y_I|\{\mathbf{u}_n^{(j)}\}, y_{1:n-1}) = \frac{\#[y_I; \{\mathbf{u}_n^{(j)}\}] + \alpha(y_I)}{N + \sum_{y_I} \alpha(y_I)} \quad (11)$$

Comparing the Bayes estimators (10) and (11) to the histogram estimator (9), it is commonly remarked that the Dirichlet prior parameters can be interpreted as *pseudo-counts*, or *pseudo-observations* whose influence diminishes as the amount of data N increases.

The notion of an “objective” prior is considerably more involved for the multinomial case [18], and over the years, several choices of $\boldsymbol{\alpha}$ have been proposed. Recent work [10] has suggested that *weak priors* are preferable for multinomial problems as otherwise the set of possible parameters for which the Bayes estimator is preferable (with respect to squared loss) to the MLE shrinks rapidly.

The strength of the prior is particularly relevant for our algorithms when some outcomes of the set are unobserved. An outcome y_I with an empirically-observed count of zero will have its probability approximated as

$$\hat{q}_n(y_I|\{\mathbf{u}_n^{(j)}\}, y_{1:n-1}) = \frac{\alpha(y_I)}{N + \sum_{y_I} \alpha(y_I)}$$

The parameter $\alpha(y_I)$ can thus be seen to control the smoothness of the estimator; larger values of α result in increased probability that the states sampled by the SCP will be unobserved in the proposal’s population, while smaller values yield increased fidelity to the empirical statistics. Hence it is undesirable to make α too large relative to N as such a choice will corrupt an inherently favorable proposal. On the other hand, some reasonable “leakage” probability to unseen states is desirable and indeed, as we shall see in Section 4.1, *required* to make the importance sampling estimators theoretically correct.

An additional appealing property of the Bayesian framework is that updating the estimators as new observed data arrive is straightforward. More precisely, suppose that we *store*, for the clamping condition $y_{1:n}$, the counts occurring in the samples $\{\mathbf{u}_n^{(j)}\}$ from a batch of N constrained process runs; if we draw another set $\{\mathbf{v}_n^{(j)}\}$ of size N from the same constrained process, we simply evaluate the updated estimator as

$$\hat{q}_n(y_I|\{\mathbf{u}_n^{(j)}\} \cup \{\mathbf{v}_n^{(j)}\}, y_{1:n-1}) = \frac{\#[y_I; \{\mathbf{u}_n^{(j)}\}] + \#[y_I; \{\mathbf{v}_n^{(j)}\}] + \alpha(y_I)}{2N + \sum_{y_I} \alpha(y_I)}$$

storing the modified set of counts for the next update. In the SCP framework, this implies that one has the option of interleaving the operations of *generating* samples from estimators available at a given time with periodic (possibly randomized) *refinement* of estimator accuracy by Bayesian updating following drawing more samples from the appropriate constrained process. This can be understood as a form of dynamical *querying* of the unknown proposal distribution.

3.3.2 Robust Bayesian Estimators

In distinction to the usage of non-informative priors, an alternative method of setting α , discussed in detail in [19] for multinomial inference, appeals to the notion of *Bayesian robustness* [2]. In the robust Bayesian framework, one considers the effect of prior misspecification on an estimator’s quality as the prior is allowed to vary within some family. This departs from the traditional Bayesian methodology but nonetheless yields estimators with appealing properties. In this work, we will present a simple and efficiently-computable estimator that is not necessarily optimal, but works well enough for the purposes of the Monte Carlo algorithms. See [19] for more sophisticated options and an in-depth discussion.

We define the *single-pseudocount family* Γ as the set of Dirichlet distributions² over outcome probabilities $\{q(y_I)\}$ whose parameters α sum to 1:

$$\Gamma = \left\{ \alpha : \sum_{y_I \in \mathcal{Y}_I} \alpha(y_I) = 1 \right\} \quad (12)$$

Assuming that the prior distribution lies within this family is not necessarily justified when the data are very sparse, i.e. most outcomes are observed to occur at most a few times. In our case however, we dynamically construct tree-based *partitions* over the set of outcomes (Section 3.3.4), which has the effect of controlling the sparsity. In that context, the family defined in (12) is quite appropriate. We note that the well-known non-informative prior due to Perks [36], with $\alpha(y_I) = \frac{1}{|\mathcal{Y}_I|}$ for all y_I , belongs to Γ .

Given an estimator of outcome probabilities, the worst-case *posterior Kullback-Leibler (KL) loss* over the priors in Γ provides a conservative measure of its reliability. In particular, suppose we construct an estimator $\hat{q}(y_I|\alpha)$ over the outcomes \mathcal{Y}_I , with $\alpha \in \Gamma$. The worst-case KL loss is then defined to be

$$\rho^*(\alpha) = \sup_{\alpha' \in \Gamma} \rho(\alpha', \alpha) \quad (13)$$

with the posterior loss

$$\rho(\alpha', \alpha) = \mathbb{E}_q \left[\log \frac{q}{\hat{q}} \right] \quad (14)$$

For priors in the Dirichlet family, (14) can be shown to be

$$\rho(\alpha', \alpha) = \sum_{y_I \in \mathcal{Y}_I} \frac{\alpha'(y_I) + \#(y_I)}{1 + N} \left[\psi[\alpha'(y_I) + \#(y_I) + 1] - \psi[1 + N + 1] - \log \frac{\alpha(y_I) + \#(y_I)}{1 + N} \right] \quad (15)$$

²We abuse notation and identify a prior distribution with its parameters

where $\psi(\cdot)$ is the *digamma function* [1]. The loss (15) represents, up to an additive constant, the posterior expected bits of divergence between the Bayes estimator under *assumed* prior $\boldsymbol{\alpha} \in \Gamma$ and the true $q_n(\cdot|y_{1:n-1})$ if the latter were *actually* a priori Dirichlet-distributed with parameters $\boldsymbol{\alpha}' \in \Gamma$; a smaller loss implies a more reliable estimator. This formulation enables an analysis of estimator robustness. The *worst-case* loss defined in Equation (13) yields the maximum divergence, over all Dirichlet priors whose parameters lie on the *standard simplex*, between the true distribution and the estimator constructed by assuming $\boldsymbol{\alpha}$. In principle, one could seek an estimator that minimized (13). Unfortunately, computing such an estimator is non-trivial, though still “tractable.” In this work, we propose a simple approximation to the Bayes estimator that would yield minimum worst-case loss over priors in Γ . Consider the empirical counts of all outcomes $\{y_I\}$, and let $\#^{(1)}$ refer to the smallest among them, for example zero. Let $\mathcal{Y}^{(1)}$ be the set of outcomes with count $\#^{(1)}$. We use a Bayes estimator as defined in (11) with parameters

$$\alpha(y_I) = \begin{cases} \frac{1}{|\mathcal{Y}^{(1)}|} & y_I \in \mathcal{Y}^{(1)} \\ 0 & \text{otherwise} \end{cases} \quad (16)$$

When there are empty outcomes, i.e. $\#^{(1)} = 0$, the probability of generating *some* outcome $y_I \in \mathcal{Y}^{(1)}$ is simply

$$\frac{1}{1+N}$$

with the individual outcomes in $\mathcal{Y}^{(1)}$ occurring uniformly.

To quantify reliability, we would like to evaluate (13) under our estimator. It can be shown that when using $\boldsymbol{\alpha}$ as prescribed in (16) the worst-case loss is achieved either when $\alpha'(y_I) = 1$ for any single member y_I of $\mathcal{Y}^{(1)}$ or for one in the set $\mathcal{Y}^{(2)}$ of those occurring with *second-lowest count*, with the rest set to zero. The maximum can therefore be computed by evaluating (15) for these two choices of $\boldsymbol{\alpha}'$ and taking the larger of the two values. By using appropriate data structures, this computation is relatively inexpensive.

The KL divergence allows natural comparison between losses on domains of *different cardinality*. Given, for example, a subset I of 4 variable indices, implying that $|\mathcal{Y}_I| = 16$, and another one J of 5 indices, so that $|\mathcal{Y}_J| = 32$, the posterior KL losses in both cases are nonetheless directly commensurable. This feature is especially relevant when we dynamically determine an approximately optimal partition of the state space subject to a loss constraint as described in the state space sampling algorithm presented in Section 5. Within a sampling context, the divergence has an additional relevant aspect: it can readily be shown by expanding the logarithm to first order that the KL divergence is approximately (half) the importance weight *variance* resulting from using the estimator as a proposal to the true distribution.

The strategy to construct a fine partition of the outcome set subject to a constraint on the KL loss, which has the interpretation of imposing a binary tree structure on the elements, is outlined in Section 3.3.4. This strategy is leveraged in the sampling algorithm of Section 5 to maximally exploit the set of heuristic samples $\{\mathbf{U}^{(j)}\}$ in the approximation construction so as to minimize the

number of required calls to the heuristic. The next section discusses variance reduction and can be skipped on first reading.

3.3.3 Variance Reduction by Rao-Blackwellised Estimators

In several commonly-encountered situations, the heuristic process follows dynamics such that the systems' individual variables are assured of being in a *local* equilibrium distribution. This is certainly so for simulated annealing, and can be straightforwardly imposed for more general processes. The property can be exploited to derive probability estimators of tremendously reduced variance, which would improve the Monte Carlo estimates yielded by our algorithm. Variants of this idea are used in several statistical applications, and are collectively referred to as *Rao-Blackwellisation* [7] due the appearance of the same principle in the fundamental Rao-Blackwell theorem of estimation theory.

In our context, the method informally consists of replacing the count-based Bayes estimators of the type discussed in (11) with ones based on averaging the *exact local probabilities*, which can be computed easily. To use the Ising model as an example, given any state $\mathbf{y} \in \mathbb{S}^m$, the local equilibrium probability of variable i is given by

$$\Pr(x_i|\mathbf{y}) = \Pr(y_i|\mathbf{y}_{\mathcal{N}(i)}) = \frac{e^{-y_i(h_i + \sum_{j \in \mathcal{N}(i)} J_{ij}y_j)}}{e^{(h_i + \sum_{j \in \mathcal{N}(i)} J_{ij}y_j)} + e^{-(h_i + \sum_{j \in \mathcal{N}(i)} J_{ij}y_j)}} \quad (17)$$

We propose constructing the Rao-Blackwellised estimator to the probability $q_n(y_I|y_{1:n-1})$ over the variable set y_I in a *top-down* manner as follows. Let $(i_1, \dots, i_{|I|})$ be a sequence consisting of the elements of I , and define the sequences

$$I_k = \begin{cases} 1, \dots, n-1 & \text{for } k = 1 \\ 1, \dots, n-1, i_1, \dots, i_{k-1} & \text{for } k > 1 \end{cases}$$

We define the (smoothed) Rao-Blackwellised estimator to be

$$\hat{q}_n^{rb}(y_I|\{\mathbf{u}_n^{(j)}\}, y_{1:n-1}) = \prod_{k=1}^{|I|} \hat{q}_n^{rb}(y_{I_k}|\{\mathbf{u}_n^{(j)}\}, y_{I_k}) \quad (18)$$

where the elements of the product in (18) are

$$\hat{q}_n^{rb}(y_{I_k}|\{\mathbf{u}_n^{(j)}\}, y_{I_k}) = \frac{\sum_j \Pr(y_{I_k}|\mathbf{u}_n^{(j)}) + \alpha(y_{I_k})}{\#(y_{I_k}) + \sum_{y_I} \alpha(y_I)} \quad (19)$$

The summation in the numerator of (19) is over all sample indices j such that variables I_k of $\mathbf{u}_n^{(j)}$ agree with the conditioning sets y_{I_k} , and $\#(y_{I_k})$ is the total number of occurrences of y_{I_k} in $\{\mathbf{u}_n^{(j)}\}$.

Due to the requirement of evaluating the conditional probabilities, the Rao-Blackwellised estimator is somewhat more costly to compute than the count-based Bayes estimator, but the corresponding improvement in accuracy can be well worth the effort, as we will show in Section 6. Indeed

we remark that for systems at very high temperature, where the multinomial sampling variance is expected to be at its maximum, the Rao-Blackwellised estimator returns almost perfect estimates of the true probabilities.

3.3.4 Dynamical Construction of a Partition

We now generalize the problem of Bayesian probability estimation to the form that will be used in the algorithm. Suppose we have clamped a set of variables and run the constrained proposal on the remaining variables with indices $I \subseteq \{1, \dots, m\}$. We seek to build a distribution on as large a portion as possible of the unconstrained state space using the samples $\{\mathbf{u}^{(j)}\}$. For readers wishing to skip the pedantic details of this section on first reading, the idea can be summarized as follows: continue branching a binary tree, whose leaf nodes represent partial states, computing an estimator for the probabilities of the tree nodes using the sample statistics, until the KL loss described in Section 3.3.2 grows unacceptably large. An example of such a tree appears in Figure 2

Consider the augmentation of full state space \mathbb{S}^m with the value \square , meaning *unassigned* (or *free*.) We define a *partial state* $\sigma \in \{+, -, \square\}^m$. For example, if $m = 4$, then $\sigma = -\square + \square$ corresponds to the binary state with variables 1, 3 set to $-$, $+$ respectively and the rest unspecified, while $\sigma = \square\square\square\square$ means no variables are assigned. Each partial state σ thus naturally defines a *binary subcube* $A(\sigma)$, i.e. a set of all binary states with some subset of the variables having fixed values. For example:

$$A(-\square + \square) = \left\{ \begin{array}{cc} -\boxed{+}\boxed{+} & -\boxed{+}\boxed{-} \\ -\boxed{-}\boxed{+} & -\boxed{-}\boxed{-} \end{array} \right\}$$

where the boxes over the instantiated variables in the subcube clarify that they were free in σ . Clearly the extreme cases of $\sigma = \{\square\}^m$ and $\sigma_i \in \{+, -\}$ for all i correspond, respectively, to subcubes of size 2^m and 1 respectively. Where there is no ambiguity, we will refer to the binary subcube $A(\sigma)$ by its corresponding partial state σ . Furthermore, we can extend our previous *count* definition to that of a partial state σ given samples $\{\mathbf{u}^{(j)}\}$ as

$$\#[\sigma; \{\mathbf{u}^{(j)}\}]$$

which returns the number of times that the specific configuration of all *assigned* variables in σ occurs in $\{\mathbf{u}^{(j)}\}$

Returning to the estimation problem, define σ_R to be the *root* partial state corresponding to all possible outcomes of the constrained proposal with free variables y_I . We desire a maximum *partition* \mathcal{A} of the subcube $A(\sigma_R)$, i.e as large a collection as possible of pairwise disjoint subcubes $\mathcal{A} = \{A_i\}$ with $\cup_i A_i = A(\sigma_R)$. The elements of the partition are the outcomes of a discrete distribution whose probabilities we wish to estimate. The limiting factor to the size of the partition is the statistical quality of the resultant estimator; if it gets too large, the quality will degrade unacceptably. We

represent the elements comprising a partition as *leaf nodes* of an *incomplete* binary tree T , i.e. one whose leaf nodes can lie at different depths from the root. The tree is also *full*: all its nodes have either zero or two children. Let ν_R refer to the root node of T . Each internal node of the tree corresponds to the union of its two children’s subcubes; hence subcubes decrease in size from the root to the leaves. Each node $\nu \in T$ is identified with partial state $\sigma(\nu)$. Furthermore, each internal (non-leaf) node is mapped to a *branch variable*, the unassigned variable in the node’s partial state that gets fixed in its two children. The branch variable of node ν is defined as $v(\nu) \in I$ with $v(\nu) = \emptyset$ if and only if ν is a leaf node. An example of such a structure, which we call a *subcube tree*, illustrating these rather natural ideas is shown in Figure 2. Readers familiar with the ideas of *branch-and-bound* algorithms will recognize that the subcube tree is simply a kind of *search tree* on a binary state space; our presentation is to emphasize the aspects that will be used in the algorithm.

To construct the tree along with the distribution over the outcomes, we begin with a trivial tree T_0 containing a single node ν_R and corresponding to the vacuous partition $\mathcal{A}_0 = \{\sigma_R\}$. We also maintain a *priority queue* \mathcal{F} which, inspired by the terminology of state space search [38, 45], we call the *frontier*. The queue initially contains only the root node, i.e. $\mathcal{F}_0 = \{\nu_R\}$. Generally, the frontier consists of leaf nodes whose partial states are considered valid for further refinement (or *branching*.) A leaf node in the tree is called *open* if it appears in the frontier. The priorities of the nodes in \mathcal{F} correspond to their ranks when the corresponding partial states are sorted by *decreasing* count $\#[\nu; \{\mathbf{u}^{(j)}\}]$, i.e. more populated partial states have a higher branching priority. Algorithms to implement priority queues are standard in computer science [9].

The algorithm thus begins. If the current frontier \mathcal{F}_i is empty, i.e. there are no further available nodes to refine, terminate the algorithm. Otherwise, *dequeue* the most populated open leaf node in the tree; in other words, ν' of highest priority is removed from \mathcal{F}_i . Next, from the corresponding partial state $\sigma(\nu')$, branch on one of the *unassigned* variables either at random, or according to some predetermined order³. We then compute the estimator over the potential new partition \mathcal{A}_{i+1} formed by removing $\sigma(\nu')$ from \mathcal{A}_i and adding $\{\sigma(\nu_+), \sigma(\nu_-)\}$, where $\sigma_v(\nu_+) = +$ and $\sigma_v(\nu_-) = -$, i.e. unassigned variable $v(\nu')$ now explicitly takes its two possible values. The estimator at any stage may be computed as described in Section 3.3.2. Specifically, for leaf nodes ν corresponding to partition \mathcal{A}_i , employ the Bayes estimator (11) with

$$\alpha(\nu) = \begin{cases} \frac{1}{|\mathcal{A}_i^{(1)}|} & \nu \in \mathcal{A}_i^{(1)} \\ 0 & \text{otherwise} \end{cases} \quad (20)$$

where $\mathcal{A}_i^{(1)}$ refers to the set of all members of \mathcal{A}_i with minimum count $\#[\nu; \{\mathbf{u}^{(j)}\}]$. Alternatively, the Rao-Blackwellised estimator discussed in Section 3.3.3 given by Equation (18) using the partition hyperparameters defined in (20) may be preferable to lower the variance.

³Branching according to some “greedy” criterion, as is done when constructing classification trees, is not suitable in the present context as it will heavily bias the probability estimates. Classification is quite a different problem from parameter estimation.

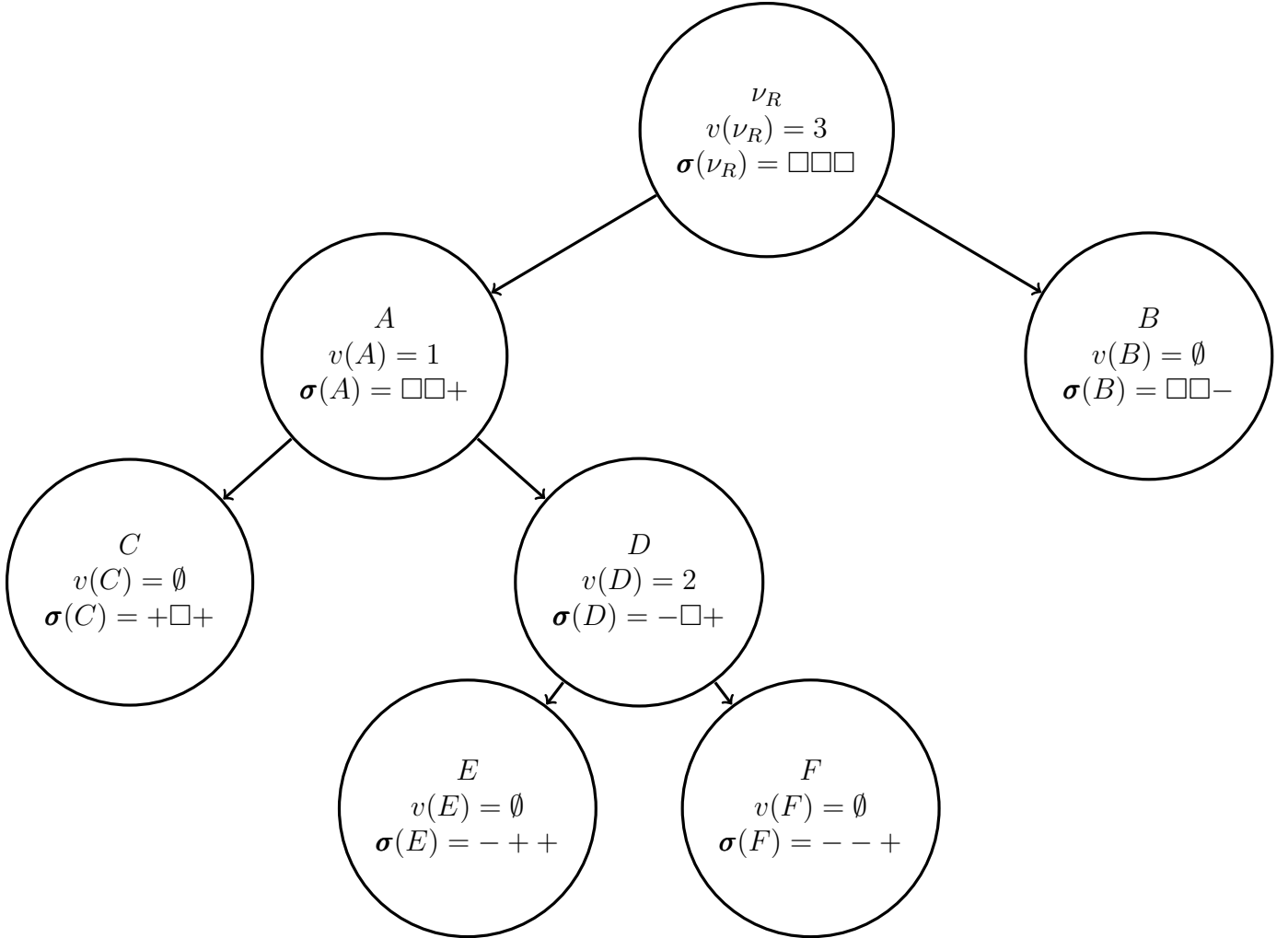


Figure 2: An example subcube tree for a state space corresponding to a problem with $m = 3$ binary variables. Each node contains the node label, its branching variable v , and its corresponding partial state σ . The symbol \square denotes an unassigned variable in the length M state. The branch variables for all leaf nodes are empty. For internal nodes, v specifies which variable is assigned in its two children. For example the left and right children A and B of root node ν_R have in their partial states variable 3 set to $+$ and $-$ respectively. Only nodes E and F correspond to fully-defined states. The state space partition \mathcal{A} represented by this tree consists of the sets of states corresponding to the leaves. In particular, $\mathcal{A} = \{+\square+, -++ , --+ , \square\square-\}$.

The cost of a partition \mathcal{A}_i is defined to be the worst-case posterior KL loss (13) computed by evaluating (15) with $\alpha'(\nu) = 1$ for an arbitrary member of $\mathcal{A}_i^{(1)}$ with the remaining $\alpha'(\nu) = 0$, evaluating it for $\alpha'(\nu) = 1$ for an arbitrary member of $\mathcal{A}_i^{(2)}$ with the rest set to zero, and taking the maximum over the two cases. Judicious application of data structures can considerably speed up this evaluation; this will not be discussed here to avoid cluttering the presentation.

If the KL cost of the potential new estimator is below the specified threshold, we accept the branch and attempt to make another refinement; otherwise, we terminate with partition \mathcal{A}_i and estimator corresponding to $\{\alpha(A_j)\}$ for the partition elements $A_j \in \mathcal{A}_i$. In the event that we continue, the children ν_+ and ν_- are only considered candidates for further branching, if, of course, they do not correspond to full binary states. Furthermore, in this algorithm, we do not allow branching into aggregations whose counts fall below a threshold. We may, for example, enforce that if $\#[\nu; \{\mathbf{u}^{(j)}\}] = 0$ for leaf node ν , then it is not eligible for further refinement. If a node is considered valid for refinement, it is *enqueued*, i.e. added by priority into \mathcal{F}_i .

We now return to the task of showing that correct Monte Carlo simulation is theoretically feasible using the SCP that uses the approximations of the type we have discussed in this section.

4 Monte Carlo Estimation via SCP

In the previous section, a method for sequential sampling from an arbitrary discrete stochastic heuristic was presented such that the resultant samples' distribution can be reasonably estimated. We have not yet discussed, however, whether usage of approximate values of the probabilities voids the statistical correctness of the standard sampling methods. We now present importance sampling and MCMC methods that are theoretically correct.

4.1 Importance Sampling

Consider first the case where one is interested in *reweighting* the samples generated by the SCP so as to allow statistical averages to be computed. This is in distinction to the *dynamical* MCMC approach that will be discussed in Section 4.2. For clarity, we will consider the one-variable-at-a-time SCP; extension to the more general cases of constructing approximations over blocks (groups) of variables and using the dynamical partitioning methods discussed in Section 3.3.4 is left as an exercise.

Suppose we have generated a population of N binary configurations $\{\mathbf{y}^{(i)}\}$ using the SCP Algorithm 1. We define the importance weight of the i^{th} sample

$$w(\mathbf{y}^{(i)}, \{\mathbf{u}_{1:m}^{(j)}\}) = \frac{\pi(\mathbf{y}^{(i)})}{\hat{q}_1(y_1^{(i)} | \{\mathbf{u}_1^{(j)}\}) \hat{q}_2(y_2^{(i)} | \{\mathbf{u}_2^{(j)}\}, y_1) \dots \hat{q}_m(y_m^{(i)} | \{\mathbf{u}_m^{(j)}\}, y_{1:m-1})} \quad (21)$$

We then have the following straightforward result.

Proposition 1. *Suppose the product of the approximating distributions $\prod_{n=1}^m \hat{q}_n(y_n | \{\mathbf{u}^{(j)}\}, y_{1:n-1}) \neq 0$ for all possible sets of $\{\mathbf{u}_1^{(j)}\}, \dots, \{\mathbf{u}_m^{(j)}\}$ wherever $\pi(\mathbf{y}) \neq 0$. Define the importance sampling estimator*

$$\hat{h} = \frac{1}{N} \sum_i w(\mathbf{Y}^{(i)}, \{\mathbf{U}_{1:m}^{(j)}\}) h(\mathbf{Y}^{(i)}) \quad (22)$$

Then (22) is an unbiased estimator of $\mathbb{E}_\pi[h(\mathbf{Y})]$.

Proof. Consider the term $w(\mathbf{Y}, \{\mathbf{U}_{1:m}^{(j)}\})h(\mathbf{Y})$ and take its expectation over all its underlying random variables:

$$\mathbb{E}[w(\mathbf{Y}, \{\mathbf{U}_{1:m}^{(j)}\})h(\mathbf{Y})] = \sum_{\{\mathbf{u}_{1:m}^{(j)}\}} \sum_{\mathbf{y}} \left[w(\mathbf{y}, \{\mathbf{u}_{1:m}^{(j)}\})h(\mathbf{y}) \prod_{n=1}^m q_n(\{\mathbf{u}_n^{(j)}\} | y_{1:n-1}) \prod_{n=1}^m \hat{q}_n(y_n | \{\mathbf{u}_n^{(j)}\}, y_{1:n-1}) \right]$$

By our assumption, w is finite for all \mathbf{y} and \mathbf{u} used to construct \hat{q} . Cancellation of the \hat{q} terms and summing out terms depending on $\mathbf{u}_{1:m}$ yields the result. \square

We now observe why Bayesian estimators are of interest in this work; their property of ensuring nonzero probability for all outcomes ensures that their support will always include that of the target π . Usage of the MLE as the approximating distributions \hat{q}_n will, in theory, lead to a biased estimator.

Proposition 22 states that the approximation is correct in expectation, but the *accuracy* of an IS estimator is typically measured by its *variance*. Although the variance of the estimator will depend on the function h , it is often instructive to consider the variance of the importance weights themselves:

$$\text{var} \left[w(\mathbf{Y}, \{\mathbf{U}_{1:m}^{(j)}\}) \right] = \sum_{\{\mathbf{u}_{1:m}^{(j)}\}} \sum_{\mathbf{y}} \frac{\pi(\mathbf{y}) \prod_{n=1}^m q_n(\{\mathbf{u}_n^{(j)}\} | y_{1:n-1})}{\prod_{n=1}^m \hat{q}_n(y_n | \{\mathbf{u}_n^{(j)}\}, y_{1:n-1})} - 1 \quad (23)$$

We observe that since $\{\hat{q}_n\}$ are assumed to be consistent estimators, i.e. $\hat{q}_n(y_n | \{\mathbf{U}_n^{(j)}\}, y_{1:n-1}) \Rightarrow q_n(y_n | y_{1:n-1})$ in probability, as we expect, the variance of w approaches that resulting from using the *exact* SCP. Unfortunately, in the case of using an arbitrary stochastic proposal as opposed to one such as MCMC enjoying asymptotic convergence properties, we cannot make a stronger statement. In particular it is not strictly true that more accurate estimates \hat{q} will result in lower overall variance. This is understandable: the proposal itself could be fundamentally poor with respect to π , in the sense that sampling from and evaluating it exactly would yield high variance. It is quite conceivable in those situations that the approximations may in fact be favourable to the exact values. This highlights an important aspect of our framework: it allows principled use of an arbitrary proposal, but it cannot compensate for an ill-fitting one. Design of an appropriate proposal is the task of the domain practitioner.

The present importance sampling framework is an especially good fit for Bayesian estimation in an additional sense to naturally solving the theoretical issue of coverage of the support of π . Suppose we possessed the capacity to *store* the approximating distributions \hat{q}_n , so that instead of building them from scratch by renewed generation from the constrained proposal prior to drawing each sample, we maintain them in memory and sample from them. Furthermore, with some specified period, we can *update* the Bayesian estimators as discussed in Section 3.3.1 by *querying* the proposal for more data. As long as we keep updating the estimates, this implies (assuming we have sufficiently

large memory) that the approximating importance sampling estimator will approach that of the SCP using its exact $q(\mathbf{y})$. Of course, “sufficiently large memory” will in general be of exponential size; Section 5 discusses our ultimate solution of performing this type of sampling by maximally exploiting finite memory resources.

We conclude this section by noting for completeness that in many cases the target π is only known up to some intractable normalization constant (or *partition function*) Z_π . Specifically, if

$$\pi(\mathbf{x}) = \frac{\tilde{\pi}(\mathbf{x})}{Z_\pi}$$

we can only evaluate $\tilde{\pi}$. In such situations, one can adapt a well-known method to dealing with this in conventional importance sampling. Define the *unnormalized* importance weights as

$$\tilde{w}(\mathbf{y}, \{\mathbf{u}_{1:m}^{(j)}\}) = \frac{\tilde{\pi}(\mathbf{y})}{\prod_{n=1}^m \hat{q}_n(y_n | \{\mathbf{u}_n^{(j)}\}, y_{1:n-1})} \quad (24)$$

The following *biased* IS estimator can then be used in place of (22):

$$\mathbb{E}_\pi[h(\mathbf{Y})] \approx \frac{\sum_i \tilde{w}(\mathbf{Y}^{(i)}, \{\mathbf{U}_{1:m}^{(j)}\}) h(\mathbf{Y}^{(i)})}{\sum_i \tilde{w}(\mathbf{Y}^{(i)}, \{\mathbf{U}_{1:m}^{(j)}\})} \quad (25)$$

Furthermore, an unbiased estimate for the partition function is given by

$$Z_\pi \approx \frac{1}{N} \sum_i \tilde{w}(\mathbf{Y}^{(i)}, \{\mathbf{U}_{1:m}^{(j)}\}) \quad (26)$$

4.2 Markov Chain Monte Carlo

We now examine the feasibility of implementing a correlated dynamical process whose equilibrium distribution is π using the SCP. In distinction to the importance sampling scenario, as long as the resultant Markov chain is *ergodic*, there is no requirement that the proposal cover the full support of π ; the process will asymptotically visit the regions of the state space with the correct probabilities. Generally, an MCMC proposal will depend on the current state \mathbf{x} but may be a large-neighbourhood generalization of local or single-site MCMC. For example one may build a *locally-modelling* distribution about the \mathbf{x} . Alternatively, one may only apply the proposal to some subset of the variables as it may not adequately cover π over the full state space.

This discussion is for reference as in the present work, we have not attempted to implement a MCMC sampling using SCP. It is nonetheless noteworthy, as in the Importance Sampling case, that usage of *approximate* distributions results in a correct methodology.

Algorithm 2 describes our MCMC routine. In contrast to IS, at each step, a single joint sample is drawn from the proposal and a random decision is made whether to accept the sample or remain

at the current point. To enforce *detailed balance* (DB), which ensures that the process converges to the correct distribution π , the probabilities of making the *forward* sampling move and its *reversal* must be computed. Neither of these two can in general be evaluated exactly for sufficiently complex heuristic proposals; in particular, note that in Algorithm 2, only the *approximate* values of the proposal are used in computing the acceptance probability α . Nonetheless, the method satisfies DB, as shown in the following.

Proposition 2. *Algorithm 2 satisfies detailed balance. In other words:*

$$\pi(\mathbf{x})q(\{\mathbf{u}\}, \{\mathbf{z}\}, \mathbf{y}|\mathbf{x})\alpha(\mathbf{x}; \{\mathbf{u}\}, \{\mathbf{z}\}, \mathbf{y}) = \pi(\mathbf{y})q(\{\mathbf{z}\}, \{\mathbf{u}\}, \mathbf{x}|\mathbf{y})\alpha(\mathbf{y}; \{\mathbf{z}\}, \{\mathbf{u}\}, \mathbf{x}) \quad (27)$$

Proof. Suppose without loss of generality that the LHS $\alpha < 1$ so that α on the RHS, corresponding to the *reverse* process of generating the sets of samples $\{\mathbf{z}_n\}$, \mathbf{x} using the approximate proposals computed using these samples, and finally the sets $\{\mathbf{u}_n\}$, is therefore 1. Then the overall forward transition probability under invariant distribution π , i.e. the LHS of (27), is

$$\pi(\mathbf{x}) \prod_{n=1}^m q_n(\{\mathbf{u}_n^{(j)}\} | y_{1:n-1}, \mathbf{x}) \hat{q}_n(y_n | \{\mathbf{u}_n^{(j)}\}, y_{1:n-1}, \mathbf{x}) \prod_{n=1}^m q_n(\{\mathbf{z}_n^{(j)}\} | x_{1:n-1}, \mathbf{y}) \times \alpha$$

which by substituting the definition of α yields

$$\pi(\mathbf{y}) \prod_{n=1}^m q_n(\{\mathbf{z}_n^{(j)}\} | x_{1:n-1}, \mathbf{y}) \hat{q}_n(x_n | \{\mathbf{z}_n^{(j)}\}, x_{1:n-1}, \mathbf{y}) \prod_{n=1}^m q_n(\{\mathbf{u}_n^{(j)}\} | y_{1:n-1}, \mathbf{x})$$

Under the assumption of $\min(1, \frac{1}{\alpha}) = 1$, we see that this is precisely the reverse transition probability from \mathbf{y} to \mathbf{x} via the $\{\mathbf{z}_n\}$ and $\{\mathbf{u}_n\}$ auxiliary variables, i.e. the RHS of (27). Hence detailed balance is satisfied over all random variables. \square

Before leaving this section, we remark that one's options for storing and modifying the proposal distribution in the MCMC setting are more limited than they are for importance sampling, where such strategies do not invalidate the algorithm. This will be discussed more thoroughly in future work examining the SCP for performing MCMC; for now, we note that Algorithm 2 requires recomputing the forward and reverse proposals for each move attempt.

5 State Space Sampling: Putting it all together

5.1 Algorithm Summary

We have presented ideas for sequentially constructing approximations to an unknown stochastic process with which we desire to sample from discrete target distribution π . We have shown that both importance sampling and MCMC are in principle feasible using the general approach. Practical

Algorithm 2 Markov Chain Monte Carlo by SCP

Given state \mathbf{x} , generate (correlated) updated state \mathbf{x}'

Draw forward sample

Sample $\{\mathbf{U}_1^{(j)}\} \sim q_1(\mathbf{u}|\mathbf{x})$

Evaluate $\hat{q}_1(y_1|\{\mathbf{u}_1^{(j)}\}, \mathbf{x})$

Sample $Y_1 \sim \hat{q}_1(y_1|\{\mathbf{u}_1^{(j)}\}, \mathbf{x})$

for $n = 2 \dots m$ **do**

 Sample $\{\mathbf{U}_n^{(j)}\} \sim q(u_{n:m}|y_{1:n-1}, \mathbf{x})$

 Evaluate $\hat{q}_n(y_n|\{\mathbf{u}_n^{(j)}\}, y_{1:n-1}, \mathbf{x})$

 Sample $Y_n \sim \hat{q}_n(y_n|\{\mathbf{u}_n^{(j)}\}, y_{1:n-1}, \mathbf{x})$

end for

Compute reverse proposal

Sample $\{\mathbf{Z}_1^{(j)}\} \sim q(\mathbf{z}|\mathbf{y})$

Evaluate $\hat{q}_1(x_1|\{\mathbf{z}_1^{(j)}\}, \mathbf{x})$

for $n = 2 \dots m$ **do**

 Sample $\{\mathbf{Z}_n^{(j)}\} \sim q_n(z_{n:m}|x_{1:n-1}, \mathbf{y})$

 Evaluate $\hat{q}_n(x_n|\{\mathbf{z}_n^{(j)}\}, x_{1:n-1}, \mathbf{y})$

end for

Acceptance step

Evaluate $\alpha = \min\left(1, \frac{\pi(\mathbf{y}) \prod_{n=1}^m \hat{q}_n(x_n|\{\mathbf{z}_n^{(j)}\}, x_{1:n-1}, \mathbf{y})}{\pi(\mathbf{x}) \prod_{n=1}^m \hat{q}_n(y_n|\{\mathbf{u}_n^{(j)}\}, y_{1:n-1}, \mathbf{x})}\right)$

Sample $R \sim U[0, 1]$

if $R < \alpha$ **then**

$\mathbf{x}' \leftarrow \mathbf{y}$

else

$\mathbf{x}' \leftarrow \mathbf{x}$

end if

matters have so far been deferred or only peripherally mentioned. In this section, we finally orchestrate the disparate components into a workable importance sampling algorithm. Generalization to MCMC will be considered in future work.

The method we propose is clearly motivated by the ideas of *state space search* [38, 45] from computer science. In that classical idea, a *heuristic function* is used to guide exploration of a state space with the objective of finding some *goal state*, for example one of minimum cost. In this work, we use our results on the statistical correctness of importance sampling with the SCP to generalize state space search to the stochastic setting, and we hence call the algorithm, somewhat insipidly, *state space sampling*(SSS). The approximate statistics gathered from runs of the proposal process will serve as the randomized heuristic decision rules. In direct analogy to the search case, the quality of the resultant estimates depend on the suitability of the proposal to the target distribution.

We will illustrate the key aspects in Section 5.2 using a running example; pseudocode describing a rudimentary version is included in Section 5.3. Here we quickly summarize the method.

An outer loop seeks to generate, say, K samples $\{\mathbf{Y}^{(i)} \in \mathbb{S}^m\}$ for use in an importance sampling estimator. Initially, no statistical model of the proposal distribution exists, so we instantiate samples $\{\mathbf{U}^{(j)}\}$ from the process and dynamically determine as large a state space partition as possible subject to a conservative constraint on the KL loss as described in Section 3.3.4. In other words, we grow a subcube tree and determine a Bayesian count-based or Rao-Blackwellised estimator over its nodes' occurrence probabilities. All leaf nodes then have nonzero probability of being visited, including those for which no samples have been observed.

We next sample a leaf node from the partial tree; if this node corresponds to a *full* binary state, we return it along with its probability⁴ and proceed to draw the next state beginning from the root of the existing tree. If, on the other hand, the leaf node corresponds to an *incomplete* state, we recursively call the constrained proposal from the partial state corresponding to the visited leaf node, growing a new subcube tree and statistical representation from the leaf node. We call this a *refresh* of a leaf node; all points in the tree that result from a renewed call to the constrained process are called *refresh points*. Once the subcube tree has been extended, the sampling resumes in this manner until a full state has been generated, which is returned along with its probability.

Due to *caching* in computer memory of the overall tree between subsequent state requests, considerable savings in the number of required proposal process runs can be achieved in some circumstances. These runs constitute the dominant computational bottleneck for problems with rough energy functions. As all leaf nodes occur with nonzero probability however, the tree will eventually grow unmanageably large as an increasing number of states are requested. To circumvent this, the subcube tree is kept at a *bounded size* by *prioritized deletion*. Once a predefined size limit is reached, the least likely elements are removed to make room for new nodes. Such memory bounding strategies have been used in state space search algorithms for some time [37]. We call an internal node both of whose children are leaves a *subleaf node*. The operation of converting a subleaf node into a leaf by deleting its two children is called *retraction*. By maintaining a *retraction priority*

⁴in practice, its logarithm to avoid numerical underflow

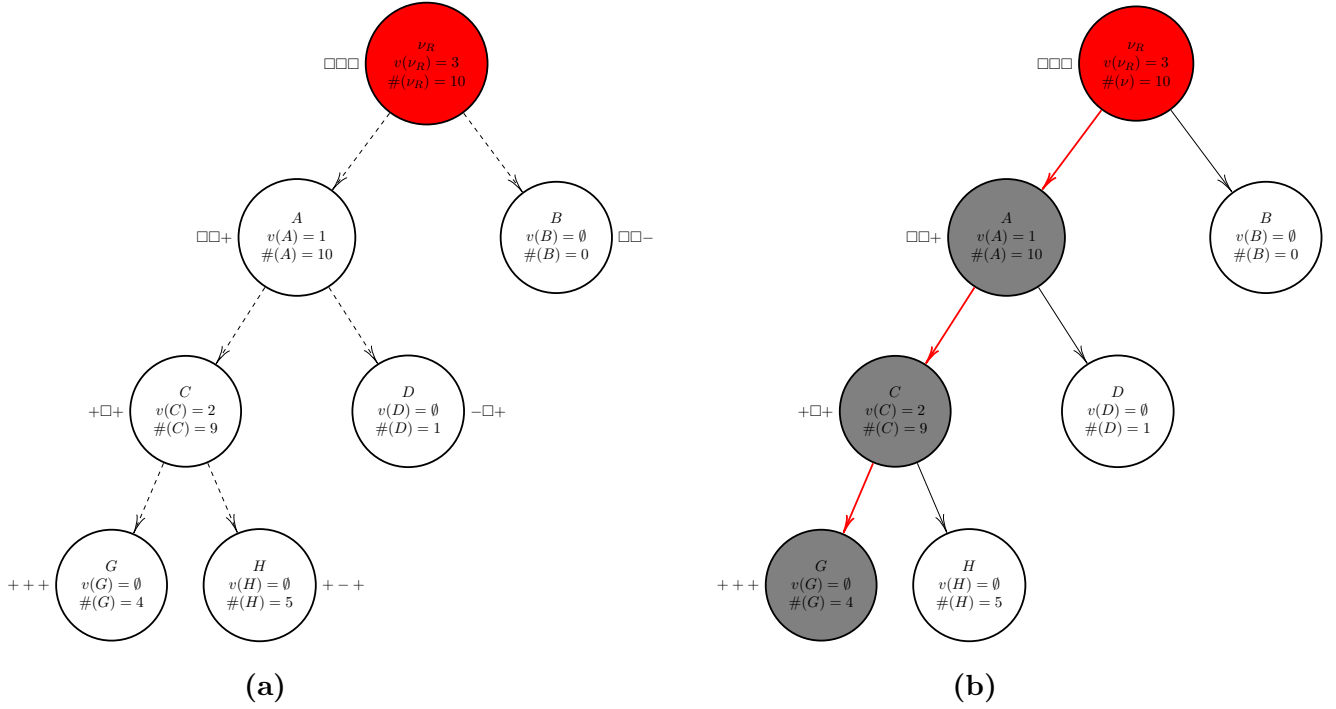


Figure 3: First stages of the procedure on a toy binary system of $m = 3$ variables. Figure 3a illustrates construction of the initial subcube tree from a population $\{\mathbf{U}^{(j)}\}$ drawn from an unconstrained proposal process. Labels, branch variables, and populations are shown in each tree node; corresponding partial binary states appear adjacently. The root node is red to signify that it is a refresh point; a maximum tree size of 9 nodes must be ensured in the subsequent algorithm. In Figure 3b, the full binary state $+++$ happens to be sampled from the model.

queue of all subleaf nodes, where a node’s retraction priority *decreases* with increasing visitation probability, we can efficiently look up candidates for retraction as a new part of the tree is grown. When the tree attains its maximum size, retraction is interleaved with branching of new nodes, so some care is required to prevent removing nodes that may interfere with the growth of a subtree. The pseudocode in Algorithm 3 illustrates the steps to ensure correct subtree construction.

5.2 State Space Sampling: The Comic Book

As promised, we now illustrate a simple run of the algorithm. We wish to generate samples on an $m = 3$ variable binary state space. All constrained proposal runs will draw the same number of samples ($N = 10$), though as discussed in Section 3.2, this is not required. To demonstrate the memory-bounding aspect, we impose a size limit on the subcube tree of 9 nodes.

Prior to drawing the first sample, we of course possess no statistical representation, hence we draw a population $\{\mathbf{U}^{(j)}\}$ from the proposal with no constraints applied. A subcube tree is constructed as shown in Figure 3a. Each tree node displays its label (e.g. ν_R for the root,) its

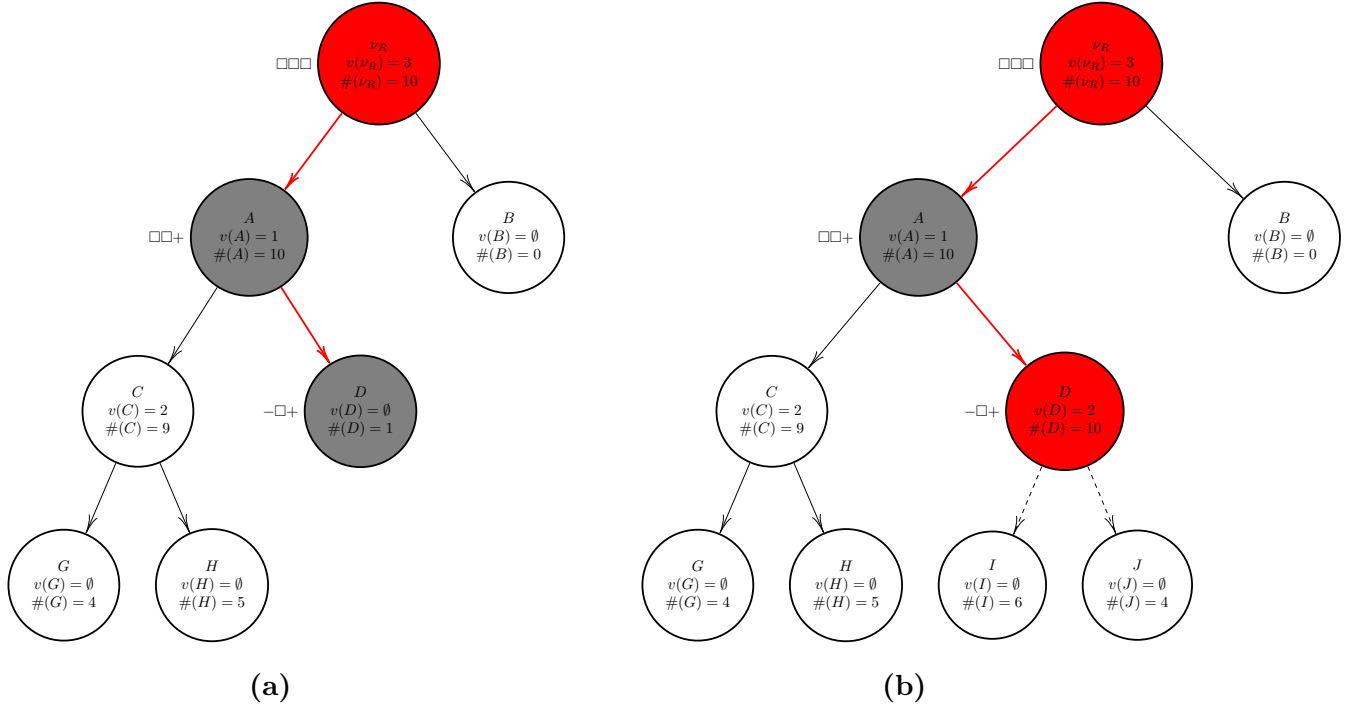


Figure 4: Figure 4a shows a sample from the subcube tree encountering leaf node D , paired with incomplete binary state $-\square+$. Hence, sampling pauses as we *query* for more data by running the proposal with constraining condition $-\square+$. The subcube tree is *extended* in Figure 4b, with node D becoming a refresh point. The tree is now at its maximum allowable size 9.

branching variable v , and the population of samples in the data with the corresponding partial state. Leaf nodes do not possess a branch variable. In Figure 3a, we indicate the partial states beside each tree node; note that only nodes G and H represent fully-instantiated states. Furthermore, node B is excluded in our algorithm from further branching because it is empty; node D was prevented from branching because it would have violated the KL loss constraint (the tree would have become unreliable.) The root node is coloured red to signify that it was a refresh point. We construct the Bayes estimator over the leaf nodes of the subcube tree as described in Section 3.3.4, where in this case the partition element of minimum count is node B , and recursively set all internal node probabilities. Node C is a subleaf node, and so it is entered into the retraction queue.

We then proceed to sample from the representation in Figure 3a; the red arrows and sequence of gray nodes in Figure 3b show the sampling of a leaf node that happens in this case to represent the full state $+++$. This state and its probability under the model can then be used in an importance sampler.

Suppose that, as shown in Figure 4a, in a later request for a sample we happen to visit node D , mapping to the incomplete state $-\square+$. The sampling pauses as *extension* of the tree is required.

In Figure 4b, node D becomes a refresh point; 10 runs of the proposal are performed with clamping condition $-\square+$. Nodes I and J are generated to extend the subtree. As a result of the extension, D becomes a subleaf and is thus placed in the retraction queue. Sampling resumes in Figure 5; the full

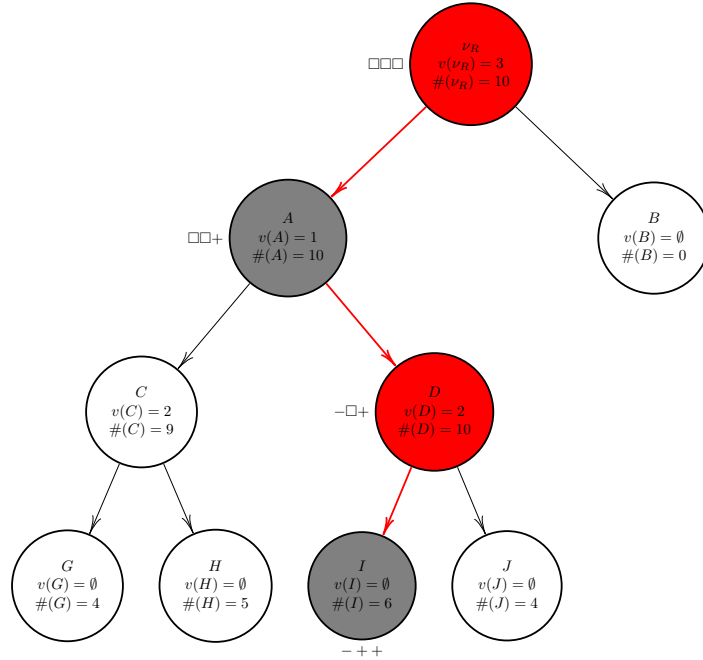


Figure 5: Continuation of the sampling paused in Figure 4a; in this case, full binary state $-+++$ results.

state $-+++$ results. Its returned probability is simply the product of the conditional probabilities along the path from the root, irrespective of which model was used to approximate the conditionals. Note that the overall number of generated nodes is now 9, so the tree is at its full capacity. Any further node generations will now require corresponding retractions.

In Figure 6a, we happen to visit node B , with partial state $\square\square-$. Once again, sampling pauses at node B while it is refreshed with a call to the proposal with condition $\square\square-$ imposed. In Figure 6b the first growth step using the new population generates nodes E and F by branching on variable $v = 2$; to enforce the tree size constraint, a subleaf node is retracted. In this case, it happens that node D has a lower visitation probability than C , so its two children I and J are deleted, maintaining the tree size at 9. Node B is a subleaf now, but is not yet considered a retraction candidate to avoid interfering with the subtree under construction.

The tree is continued from F to yield nodes M and N in Figure 7a. The sole remaining subleaf, node C , is retracted, rendering A a subleaf. But the refresh from B is now complete (E is empty.) All subleaves of the new subtree are now considered eligible for retraction; in this case, F is enqueued. The sampling which paused at B in Figure 6a now resumes; Figure 7b shows the continuation to node M , i.e. full state $-+++$.

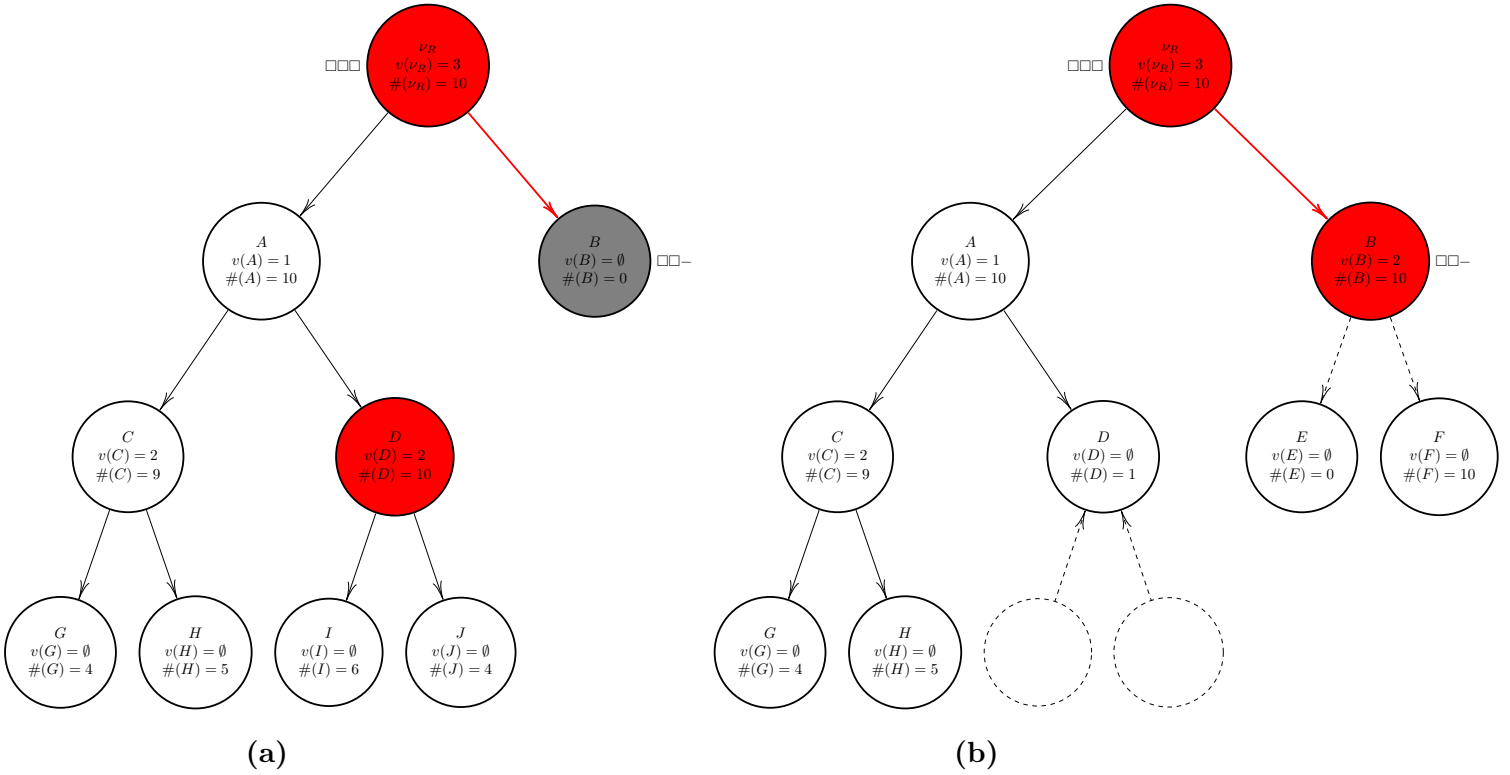


Figure 6: Incomplete state $\square\square-$ is sampled in 6a; a refresh is performed from node B , but extension of the tree now requires retraction to respect the 9 node size restriction. Of the two eligible *subleaf* nodes, i.e. those with two children, both of which are leaves, node D happens to have a higher priority for retraction because it has a lower visitation probability. Nodes I and J are thus deleted to make room for E and F .

Having illustrated the essential ideas, we next present pseudocode of a variant of SSS that was used in our experimental validation.

5.3 Algorithm Pseudocode

The collection of functions comprising SSS is presented in Algorithm 3. The pseudocode must necessarily trade off transparency of presentation with efficiency of implementation; we certainly do not claim that the routines are optimal. Not every variable and function in the pseudocode is explicitly defined; we hope that, in conjunction with the example run discussed in Section 5.2 and the discussion of the algorithm principles throughout the paper, what the methods are doing will be clear from the context. We ask the reader to mind the distinction between a node ν and a branch variable v . Following a standard convention, elements of a data structure are referred to by their name preceded by a period; for example the left child of a tree node ν is $\nu.\text{LeftChild}$.

The code presented computes the estimated state probabilities using the count-based robust

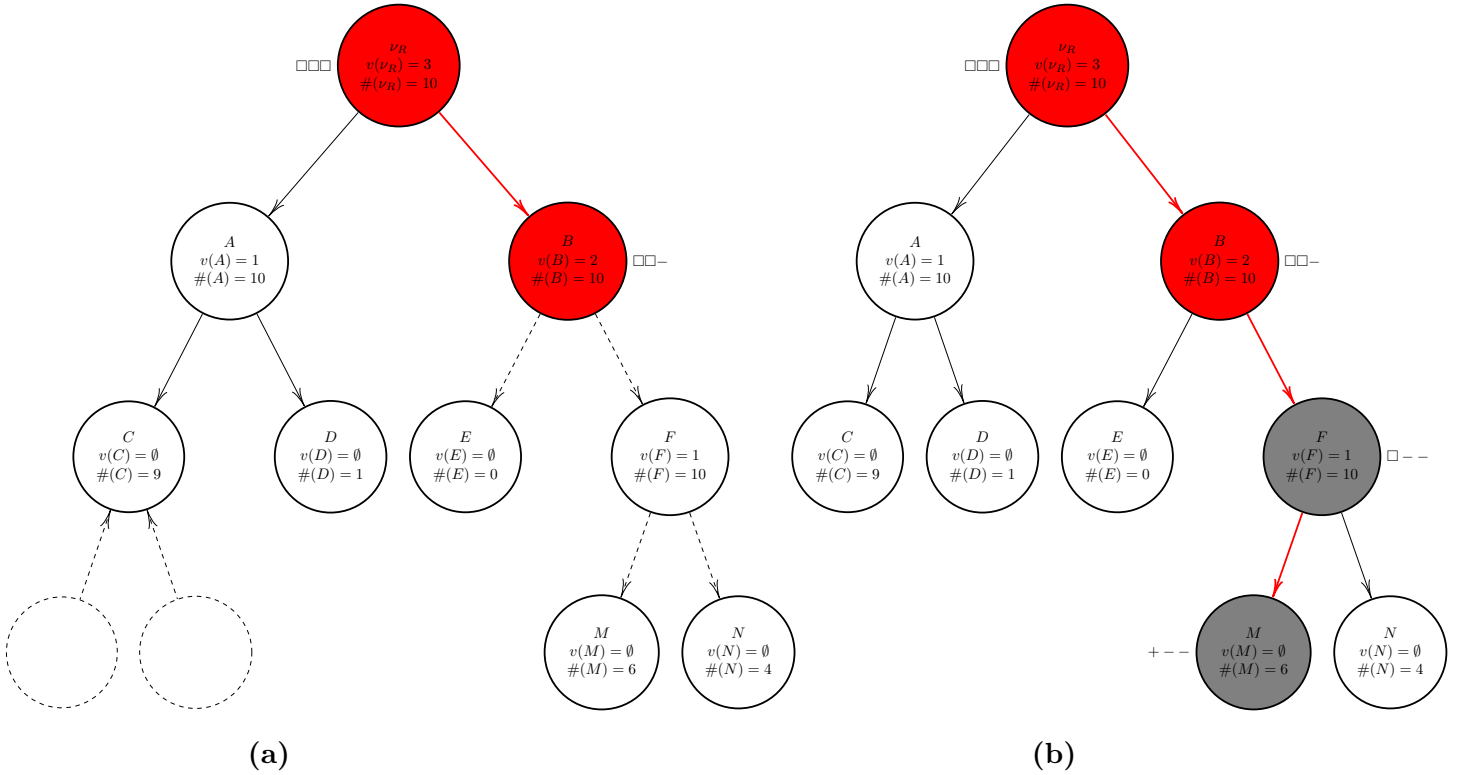


Figure 7: Extension of the tree begun in 6b continues, still using the proposal samples generated from node B . Subleaf C is retracted to free memory. At this point the extension is complete, and the sampling paused in Figure 6a resumes to generate state $+ - -$

Bayes estimator described in Section 3.3.2; extension to Rao-Blackwellisation as discussed in Section 3.3.3 is not difficult.

The main function is `SAMPLES`, which recursively returns discrete states and their (log) probabilities. It takes as input a tree node ν , a structure called `status` containing dynamical data related to the generation process, and a structure called `params` containing the user-specified simulation parameters. The `status` structure is used to track the state under construction and its log probability.

Once a call to `SAMPLES` arrives at a leaf node corresponding to an incomplete partial state, the function `EXTENDTREE` performs the required tree extension. This involves running the SCP with the user-specified heuristic process `params.simulationProcess` and constructing a robust Bayes estimator on a state space partition derived from the SCP samples $\{\mathbf{u}^{(i)}\}$. An *expansion queue* prioritizes the order in which to branch the tree nodes; variables are selected from the unassigned set $\nu.\text{freeVariables}$ according to some rule called `CHOOSEBRANCHVARIABLE`. Examples of such a branching rule are to follow a fixed or totally random order, or for problems with a topological structure, to employ a parallelisation strategy as discussed in Appendix 9.1. For Ising-type problems,

an additional possibility which we used in our implementation is to allow a randomized order, but only from among unassigned variables neighbouring those in the assigned set.

Extension of the tree terminates when the posterior KL loss exceeds threshold θ ; nodes are only considered candidates for branching if the population of the corresponding partial states is larger than $\#_{thresh}$. The function `RETRACTWORSTSUBLEAF` bounds the tree size at specified value `maxTreeSize` by prioritized deletion from a *retraction queue* of subleaf nodes.

Before presenting numerical results, we mention that the possibility alluded to in Section 4.1 of periodic Bayesian estimator updating following drawing more SCP samples from the partial state distributions corresponding to subtrees was left to future work. The idea is briefly touched upon in Appendix 9.3.

6 Experimental Results

6.1 Overview

We now turn to an experimental validation of the SSS methodology. We analyze the algorithm on four different classes of Ising model by running a simulated annealing (SA) process under varying sets of heuristic parameters. The analytically-solvable cases of *independent* and *chain-structured* (one-dimensional) Ising variables are considered, as are the more complex *fully-connected* (or *Sherrington-Kirkpatrick*) and *three dimensional* models.

Given that one of the stated points of this work is to allow for equilibrium sampling using processes that do not necessarily converge to the target distribution, it may seem unsatisfying that we have chosen to use SA as the heuristic in demonstrating SSS. We defend the choice in this preliminary work by noting that the SSS algorithm is *agnostic* to the particular heuristic chosen, but that using an equilibrating process like SA is an informative *diagnostic* of how well SSS is performing. Recall that when using SA, each SCP run will converge to the conditional Boltzmann probability of the free variables given the constraining set. Consequently, it should be possible to show the degree of convergence of the final SSS distribution to the Boltzmann target. We make the cautionary reminder however, that strictly speaking, this does *not* show convergence of a conventional (unconstrained) SA run, from which statistics are gathered only to build the initial portion of the state space tree. The overall SSS distribution generally depends strongly on the simulation parameters of each call in the sequence used to construct the tree. In particular, if SA is run with the *same* simulation length (number of sweeps) for each clamping condition, as was done here for simplicity, the final distribution will tend to be *closer* to the Boltzmann distribution than the one arising from a plain SA run. The reason is quite simple and was touched upon in Section 3.2; as the simulated subproblems decrease in size with increased variable clamping, local equilibration on the subproblems becomes more rapid. Nonetheless, convergence to the target π when using SA within SSS *does* (asymptotically) occur, justifying SA as a natural preliminary benchmark case for our algorithm. It is reasonable to wonder if, for example, the sources of statistical error arising

Algorithm 3 State Space Sampling

```
function SAMPLES( $\nu$ , status, params)
  if status.State is a full state then
    status.logQ  $\leftarrow$   $\nu$ .logQ
    return
  end if
  if  $\nu$  is a leaf node then
    extendTree( $\nu$ , status, params)
  end if
   $\nu_{next} \leftarrow$  sampleChild( $\nu$ )
  if  $\nu$ .LeftChild =  $\nu_{next}$  then
     $S_{next} \leftarrow 1$ 
  else
     $S_{next} \leftarrow -1$ 
  end if
  status.State[ $\nu.v$ ]  $\leftarrow S_{next}$ 
  sampleS( $\nu_{next}$ , status, params)
end function
```

```
function SAMPLECHILD( $\nu$ )
   $\triangleright$  Only valid for internal nodes
   $P_+ \leftarrow \exp(\nu$ .LeftChild.logQ  $- \nu$ .logQ)
  Sample  $R \sim U[0, 1]$ 
  if  $R < P_+$  then
    return  $\nu$ .LeftChild
  else
    return  $\nu$ .RightChild
  end if
end function
```

```
function SETTREEPS( $\nu$ ,  $N$ , logQ $_r$ )
  if  $\nu$  is a leaf then
     $\nu$ .logQ  $\leftarrow \log[\#(\nu) + \alpha(\nu)] - \log(1 + N) + \log Q_r$ 
    return
  else
    setTreePs( $\nu$ .LeftChild,  $N$ , logQ $_r$ )
    setTreePs( $\nu$ .RightChild,  $N$ , logQ $_r$ )
     $\nu$ .logQ  $\leftarrow \log[\exp(\nu$ .LeftChild.logQ) +  $\exp(\nu$ .RightChild.logQ)]
  end if
end function
```

Algorithm 4 State Space Sampling (cont'd)

```
function EXTENDTREE( $\nu$ , status, params)
   $\triangleright \nu$  is root node of subtree being grown
  if  $\nu$  is not root then  $\triangleright$  Avoid root Node
    if  $\nu$ .Parent is a subleaf node then
      Remove  $\nu$ .Parent from status. $\mathcal{R}$ 
    end if
  end if
   $\{\mathbf{u}^{(i)}\} \leftarrow$  params.simulationProcess( status, params )  $\triangleright$  Sample from process
   $\nu.n \leftarrow |\{\mathbf{u}^{(i)}\}|$   $\triangleright$  Number of samples may be determined by the heuristic
   $\mathcal{F} \leftarrow$  newExpansionQueue
  enqueue( $\nu$ ,  $\mathcal{F}$ )
  while  $\mathcal{F}$  is not empty do  $\triangleright$  There exist frontier nodes
    retractionFailed  $\leftarrow$  retractWorstSubleaf(status, params,  $\nu$ .Parent)
    if retractionFailed then
      break
    end if
     $\nu' \leftarrow$  dequeueBest( $\mathcal{F}$ )  $\triangleright$  Most populated tree node is selected for branching
     $v' \leftarrow$  chooseBranchVariable( $\nu'$ ,  $\{\mathbf{u}^{(i)}\}$ )  $\triangleright$  E.g. randomly from unassigned variables
    branchTree( $\nu'$ ,  $v'$ ,  $\{\mathbf{u}^{(i)}\}$ )  $\triangleright$  Node  $\nu'$  is extended by branching on  $v'$ 
     $\alpha' \leftarrow$  robustBayesEstimator( $\nu$ )  $\triangleright$  New potential  $\alpha$  matching extended tree
     $KL \leftarrow$  evalKLCost(  $\nu$ ,  $\alpha'$  )
    if  $KL >$  params. $\theta$  then  $\triangleright$  Reject the branch on  $v'$ 
      retractTree( $\nu'$ )
      break
    end if
     $\alpha \leftarrow \alpha'$   $\triangleright$  Accept the new estimator at the leaf nodes
    if  $|\nu'.freeVariables| >$  1 then  $\triangleright$  Did we assign last possible variable?
       $\nu_+ \leftarrow \nu'.LeftChild$ 
       $\nu_- \leftarrow \nu'.RightChild$ 
      if  $\#(\nu_+) >$  params. $\#_{thresh}$  then  $\triangleright$  Only if  $\nu_+$  is sufficiently populated
        enqueue( $\nu_0$ ,  $\mathcal{F}$ )
      end if
      if  $\#(\nu_-) >$  params. $\#_{thresh}$  then  $\triangleright$  Only if  $\nu_-$  is sufficiently populated
        enqueue( $\nu_1$ ,  $\mathcal{F}$ )
      end if
    end if
  end while
```

Algorithm 5 State Space Sampling (cont'd)

setTreePs($\nu, \nu.n, \nu.\log Q$) \triangleright Recursively set internal probabilities of new subtree
updateRetractionQueue(ν, status) \triangleright Enter subleaves of new subtree into retraction queue
end function

function ROBUSTBAYESESTIMATOR(ν)

$\#_{min} \leftarrow \infty$

for $\nu' \in T(\nu)$ **do** \triangleright All nodes in subtree rooted at ν

if ν' is a leaf node **then**

if $\#(\nu') < \#_{min}$ **then**

$\#_{min} \leftarrow \#(\nu')$

end if

end if

end for

for $\nu' \in T(\nu)$ **do**

if ν' is a leaf node **then**

if $\#(\nu') = \#_{min}$ **then**

$\alpha(\nu') \leftarrow 1/\#_{min}$

else

$\alpha(\nu') \leftarrow 0$

end if

end if

end for

end function

Algorithm 6 State Space Sampling (cont'd)

```
function UPDATERETRACTIONQUEUE( $\nu$ , status)
  if  $\nu$  is a leaf then
    return
  else if  $\nu$  is a subleaf then
    enqueue( $\nu$ , status. $\mathcal{R}$ )
    return
  else
    updateRetractionQueue( $\nu$ .LeftChild, status)
    updateRetractionQueue( $\nu$ .RightChild, status)
  end if
end function
```

```
function RETRACTWORSTSUBLEAF(status, params,  $\nu_{protected}$ )
   $\triangleright$ If tree size at limit, try to delete worst subleaf, avoiding  $\nu_{protected}$ 
   $\triangleright$ If no subleaves are available to retract, returns failure
  if status.treeSize > params.maxTreeSize then
    if status. $\mathcal{R}$  is not empty then  $\triangleright$  Available nodes to retract?
       $\nu_{worst} \leftarrow$  deQueueWorst(status. $\mathcal{R}$ )
      retractTree( $\nu_{worst}$ )  $\triangleright$  Delete the two children of  $\nu'$ 
      status.treeSize  $\leftarrow$  status.treeSize - 2
      if  $\nu_{worst}$ .Parent is now a subleaf and is not  $\nu_{protected}$  then
        enqueue( $\nu_{worst}$ .Parent, status. $\mathcal{R}$ )
      end if
      return Success
    else  $\triangleright$  No available retractions
      return Failure
    end if
  else  $\triangleright$  Tree not at full capacity, no retraction needed
    return Success
  end if
end function
```

from constructing models to the heuristic distribution are large enough to severely increase the importance sampling variance. Hence, by demonstrating correct performance under SA, one can be more confident that when using another heuristic, failure of the algorithm is a signature of an inappropriate heuristic, not of errors inherent to the SSS method. When we mention “convergence of SA” in the following results, we intend it as a shorthand for “convergence of the SSS distribution under SA” with the preceding caveat in mind.

An exploration of the relative performance of the vast set of possible heuristics is a substantial undertaking and will be dealt with in future work.

As the Boltzmann distribution is sought by the SA Markov chains, it is natural to compare when possible, $\log \hat{q}(\mathbf{y})$, the log probability of each state \mathbf{y} returned by SSS, with that of $\log \pi(\mathbf{y}) = -E(\mathbf{y}) - \log Z_\pi$. Of course, $\log Z_\pi$ is not always available, but in such cases one can heuristically assess Markov chain convergence by using an estimate of Z_π . The *scatterplot* of the samples’ energies against their log probabilities yields visually useful information on the extent to which the target distribution has been reached. Ideally, $\log \hat{q}$ will be a strict linear function of E , with slope -1 (or $-\beta$ if the energy is scaled independently) and an intercept of $-\log Z_\pi$. We call this relation the *Boltzmann line*. The fidelity of the SSS samples’ E versus $\log \hat{q}$ scatterplot to this line determines the accuracy of an importance sampling estimator based \hat{q} . For example excessive variance about the relation implies that samples with very similar energies relative to the temperature, which ought to occur with nearly identical probability, will contribute quite differently to the estimator compensate for their relative difference in actual probability. In essence, this reduces the *effective* number of samples and hence the estimator’s reliability.

6.2 Methodological Details

We implemented SSS following the algorithm description in Section 5.3. Both count-based and Rao-Blackwellised estimation were allowed for. For all simulations, the SCP used $N = 2000$ samples from the heuristic to construct the dynamic state space tree; the posterior KL loss was bounded at a threshold value of $\theta = 0.05$ nats. No Bayesian updating was performed; the tree size was bounded at a maximum of 10^5 nodes by prioritized retraction of low-probability nodes. The branching rule employed for tree construction was to select a random unassigned variable from among those that neighbour assigned variables (or a totally random variable if none have been assigned.)

The *independent* (**IsingIndep**), *one-dimensional* (**Ising1D**), and *full-connected* (**IsingSK**) models all had $m = 100$ variables; the *three-dimensional* (**Ising3D**) problem was of size $m = 6 \times 6 \times 6 = 216$ nodes with periodic boundary conditions. The systems are all of relatively modest size, but this was necessitated by the lengthy simulation times when given a serial implementation such as ours. An implementation exploiting the trivially parallel nature of the population simulation, as well as the parallelism inherent to the topology of problems such as **Ising3D** as described in Section 9.1, will yield enormous speedups. The results we present nonetheless show the considerable power of the method: using a relatively simple idea, we can resolve the probabilities of states generated by a generic stochastic process with fairly high precision, despite these states occurring with extremely

small probability.

Problem `IsingIndep` was generated by sampling local fields h from a unit variance, zero mean Gaussian: $h_i \sim N(0, 1)$. All other problems had zero local field. For `Ising1D` and `Ising3D`, $J_{ij} \sim N(0, 1)$ for edges $\{i, j\}$ in the model, while with `IsingSK`, $J_{ij} \sim N(0, 1/\sqrt{m})$ for all $\{i, j\}$. The SA simulation parameters were chosen in a problem-dependent manner as described in the following section.

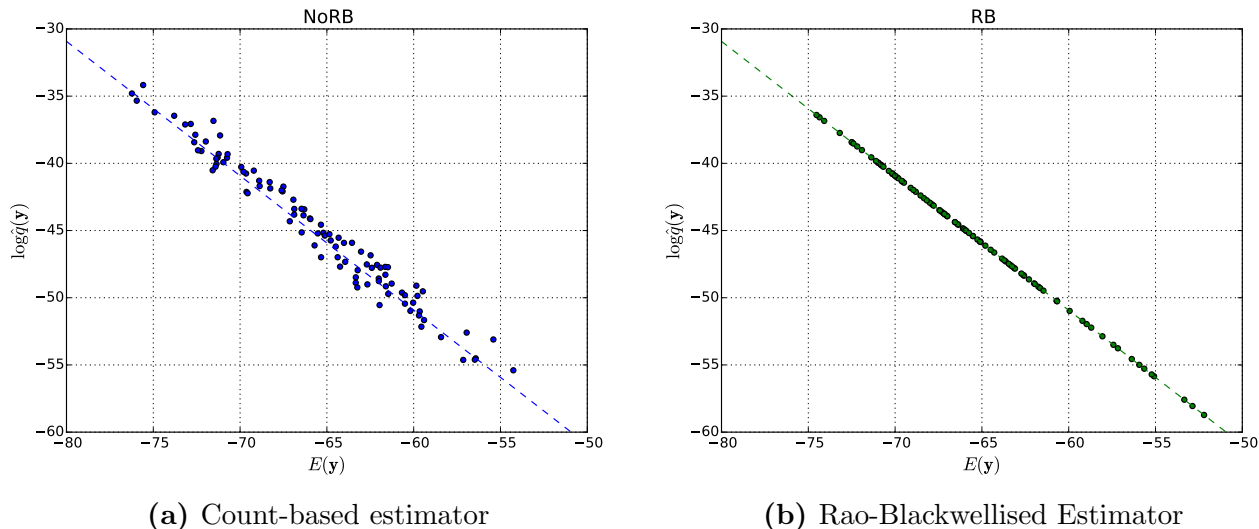


Figure 8: Scatterplot of configuration energies against log probabilities for $N_{draws} = 100$ samples generated using SSS as described in the text on the independent-spin Ising model (`IsingIndep`). The “heuristic” in this case was an exact sampler from the target distribution. The dotted line, termed the *Boltzmann line* in this text, shows where the points would ideally lie. Figure 8a shows the results using a count-based robust Bayesian estimator, while 8b uses Rao-Blackwellisation, which for this case, completely eliminates the sampling noise as expected. However even for the results using the count-based estimator, the importance weight variance with respect to the exact true distribution is a fairly modest value of ≈ 0.927 . This is noteworthy considering the minuscule probabilities of the events themselves, which were evaluated using a relatively tiny number of samples from the distribution. Direct resolution of these events, whose probabilities are down to $\sim e^{-55}$ for this ensemble, is infeasible.

6.3 Results

We first consider the `IsingIndep` case. This is a very simple problem from which sampling exactly merely requires simulating m independent Bernoulli variables. Nonetheless, SSS does not make use of this simplifying structure, and hence comparison with the known, exact values of the samples’ probabilities serves as a good initial illustration of the reliability of the algorithm with a reasonable set of parameters, as well as of the strength of Rao-Blackwellisation. The inverse temperature for this system was taken as $\beta = 1$, and exact samples were generated to construct the state space tree. The results, shown in Figure 8, show the scatterplot of the energies of $N_{draws} = 100$ samples

queried from the state space tree using count-based and Rao-Blackwellised estimators; the dotted line with slope of $-\beta$ and intercept of exactly-calculated $\log Z_\pi$ in the two subfigures show where exact samples taken from the Boltzmann distribution should lie. As expected, Rao-Blackwellisation eliminates statistical variance, but it should be noted that despite the sampling noise, *merely using the configuration statistics* can yield quite reliable estimates of the log probabilities. The states appearing in Figure 8a occur with probabilities on the order of e^{-50} ; directly approximating their values with, for example a simple histogram is simply out of the question. The importance weight variance⁵ for the count-based estimator is ≈ 0.927 , quite a modest value considering the vanishingly small probabilities being dealt with. This variance can be reduced by increasing the population size N and decreasing the posterior KL threshold θ used in constructing the state space tree. In general, the Rao-Blackwellised estimator will not eliminate the variance as it does in this simple case, but as it is not costly to compute and usually yields substantial variance reduction, it is used in all subsequent experiments.

⁵not the variance of the log of the weights

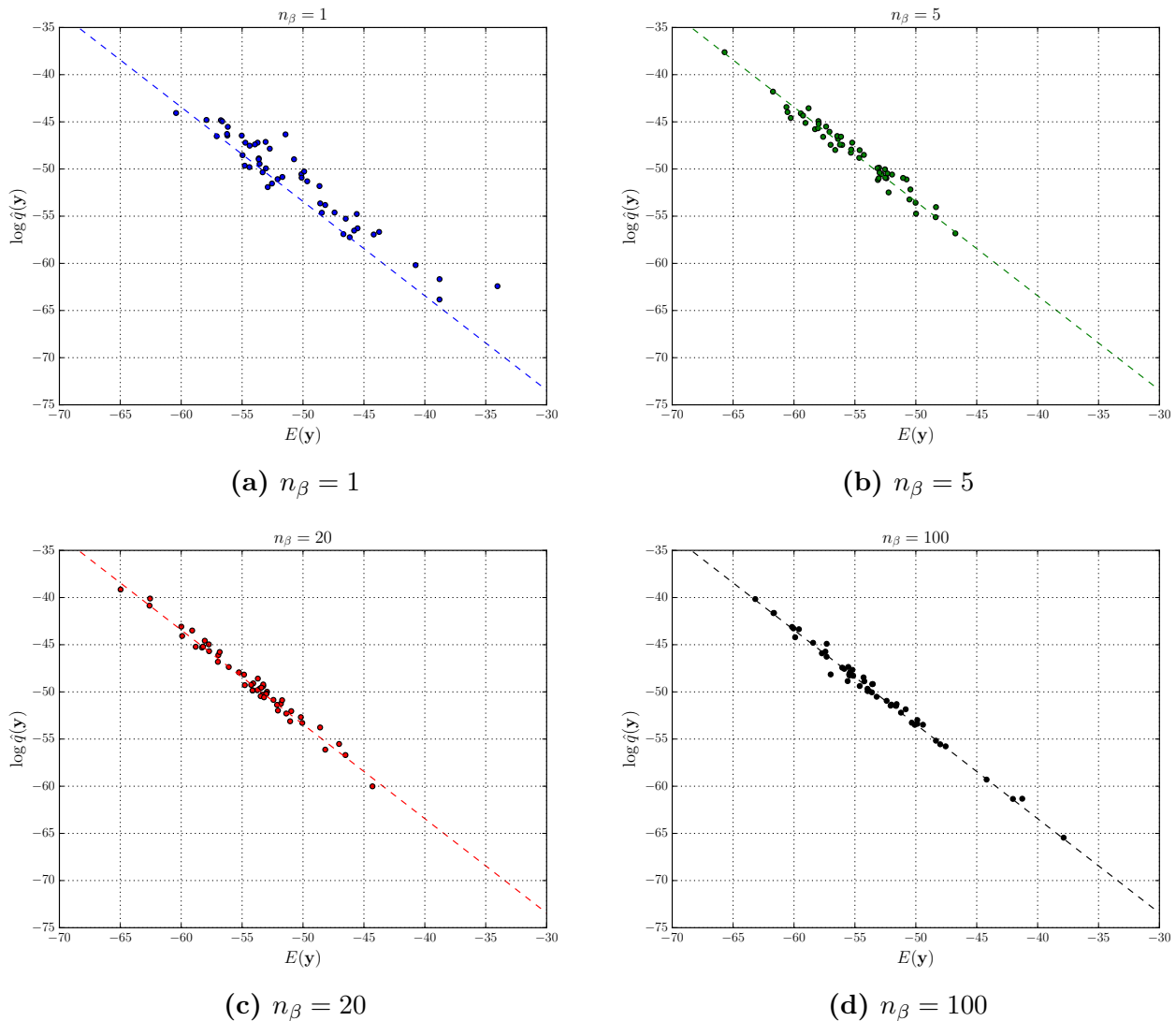


Figure 9: E versus $\log \hat{q}$ scatterplot of $N_{draws} = 50$ states generated by SSS using simulated annealing (SA) on the one dimensional Gaussian J_{ij} Ising model (**Ising1D**). The number of SA sweeps used to anneal β from 0.1 to 1 is stated below the corresponding plot. As expected, as the number of sweeps increases, the samples increasingly lie on the Boltzmann line, indicating that \hat{q} is converging to π . See text for more details.

The next set of experiments examines **Ising1D**. The target inverse temperature was set at $\beta = 1$. Due to its low treewidth, this model is still tractable in the sense that both exact sampling from its equilibrium distribution and partition function computation are straightforward. However to show some interesting behaviour, we instead run SA on this model for a set of varying simulation lengths. Interestingly, due to the continuity of J_{ij} leading to so-called “kinks”, there exist many local minima for this problem [32]. The SSS methodology allows us to monitor the nonequilibrium statistics of

the SA samples. We performed SSS using a set of $n_\beta \in \{1, 5, 20, 100\}$ simulated annealing sweeps with a linearly-increasing inverse temperature schedule beginning with $\beta = 0.1$ (the case of $n_\beta = 1$ was simply a single simulation sweep at the final temperature). SSS was called $N_{draws} = 50$ times per simulation length. The results for these four SA regimes are shown in Figure 9. As was the case for `IsingIndep`, the exact partition function was computed via dynamic programming (or the *transfer matrix* method), and the Boltzmann line is shown in each plot. We see clearly in Figure 9a that a single Monte Carlo sweep at the target temperature is enough to bring the population quite close to the Boltzmann distribution, but not quite enough to reach it. The population statistics are quite varied at this point, as we would expect from such a short simulation run. Five and 20 sweeps, as shown in 9b, move the set further towards the Boltzmann line, while after $n_\beta = 100$ sweeps (Figure 9d) many of the samples start to lie right on the line.

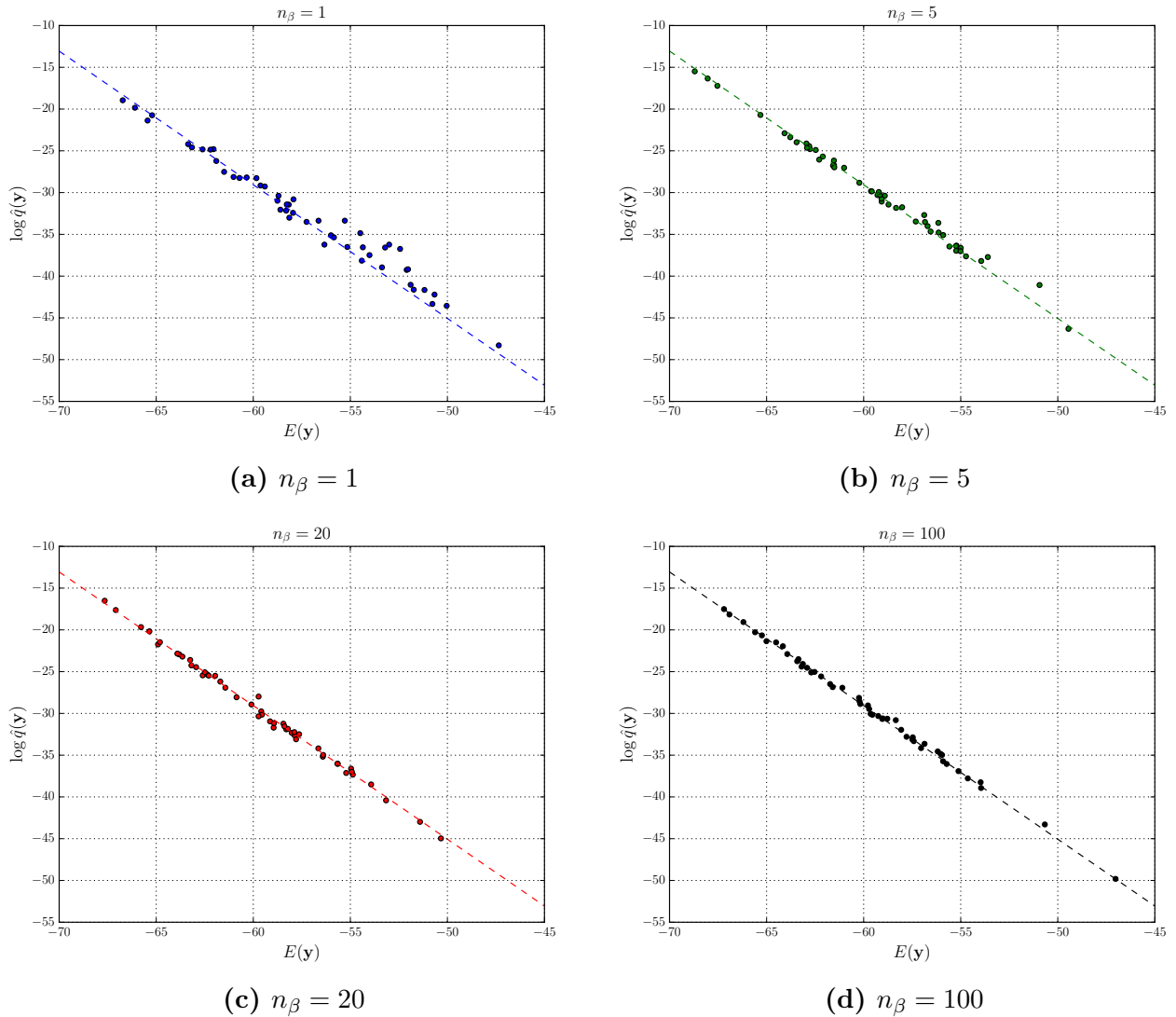


Figure 10: E versus $\log \hat{q}$ scatterplot of $N_{draws} = 50$ states generated by SSS using simulated annealing (SA) on the *fully-connected* Gaussian J_{ij} Ising model (**IsingSK**). For this instance, SA was run for each of a set of n_β batches of 6 sweeps, during which β was linearly increased from 0.1 to 1.6; n_β is indicated below each graph. We see the same expected pattern of convergence of \hat{q} to the distribution with increasing n_β . See text for details.

We proceed next to two examples for which it is no longer possible to compare against analytical results. The first of these is the 100-variable fully-connected problem **IsingSK**; β was set to 1.6, corresponding to a temperature below the spin glass transition temperature [5]. As for the case of **Ising1D**, a set of increasing SA lengths were compared against each other. We considered linearly increasing beta from an initial value of $\beta = 0.1$ to $\beta = 1.6$ over the course of $n_\beta \in \{1, 5, 20, 100\}$ steps, but as this problem is more computationally-demanding than the previous two considered,

each step consisted of 6 sweeps. Figure 10 shows the outcomes. Plotting the Boltzmann line required an estimate of $\log Z_\pi$, which was obtained with the importance sampling estimator (26) using the SSS samples under the $n_\beta = 100$ regime; the target value of $\beta = 1.6$ defined the slope. We stress that the line was *not* obtained by linear regression, lessening the chance that a seemingly good relation is an overfitting artifact. The plots show the same pattern of convergence of the samples to π . Following a single set of sweeps at the target β , the system has relaxed to the Boltzmann line, but substantial variance still exists. The fit improves as the number of SA steps increases, until $n_\beta = 100$ appears to yield an essentially converged final distribution. The reader is once again asked to note that SSS is returning individual configurations with quite accurate probability estimates across a range of many orders of magnitude (between $\sim e^{-15}$ and $\sim e^{-50}$ for this case.)

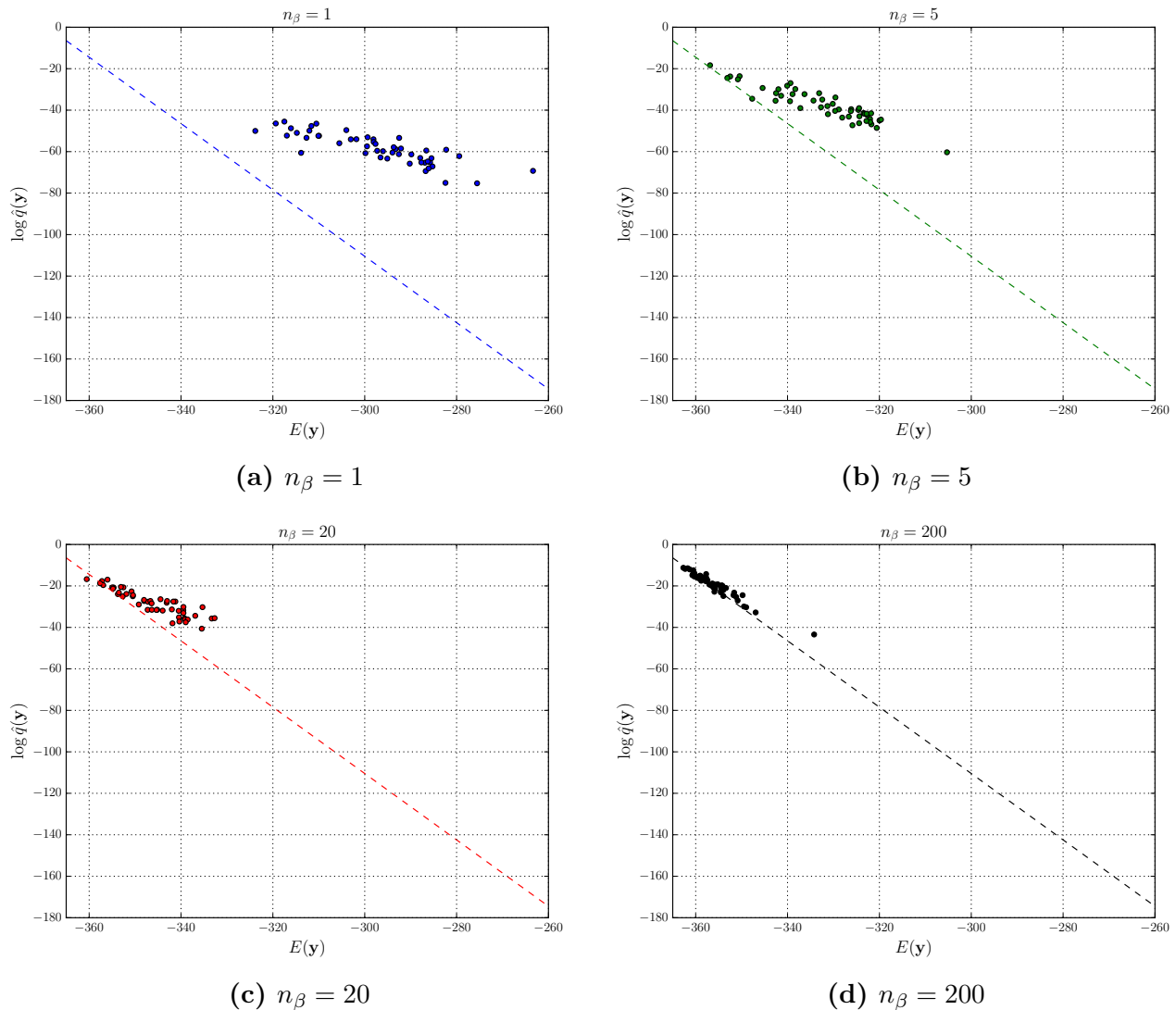


Figure 11: E versus $\log \hat{q}$ scatterplot of $N_{draws} = 50$ states generated by SSS using simulated annealing (SA) on the *three dimensional* Gaussian J_{ij} Ising model (**Ising3D**). As for **IsingSK**, SA was run for each of a set of n_β batches of 6 sweeps, with linear β increase from 0.1 to 1.6. Due to the relative difficulty of the problem, the longest run used $n_\beta = 200$. This problem exhibits hallmarks of slow SA convergence; the short runs display severe deviation from the Boltzmann line, which, unsurprisingly, becomes milder as the run is lengthened. Even the longest cannot be said to have fully converged, but in this situation one may expect importance sampling to yield satisfactory estimation.

Our final problem, the three dimensional model **Ising3D**, shows most dramatically how the sample statistics can depend on the simulation parameters and the relative difficulty SA begins to have. The set of SA steps was in this case $n_\beta \in \{1, 5, 20, 200\}$, with as before, each step consisting of 6 sweeps. Annealing was performed by increasing β linearly from 0.1 to 1.6, which again

corresponds to being below this model’s glass transition temperature [31]. The longest simulation used $n_\beta = 200$ instead of $n_\beta = 100$ as was done for the previous instances because this problem was more challenging, and equilibration seen to be relatively slow. The Boltzmann line intercept ($-\log Z_\pi$) was approximated using the longest simulation as it was for `IsingSK`. The results are shown in Figure 11. After $n_\beta = 1$ batches of SA sweeps, the ensemble exhibits considerable deviation from the Boltzmann line. While convergence to a linear relation appears to have commenced, the slope of the relation seems to suggest a higher than correct temperature and its intercept is quite at odds with the target value. Furthermore, a substantial variance exists. Over the course of $n_\beta = 5, 20$ and 200 SA sweep batches, the ensemble begins migrating to the Boltzmann line. Note that even for the $n_\beta = 200$, i.e. 1200 SA sweeps, considerable discrepancy still exists, and one would be cautious in pronouncing the system to have equilibrated. Nonetheless, importance sampling can be used to perform estimation at this point.

We close this section by cautioning that convergence of the E versus $\log \hat{q}$ relation to the Boltzmann line constructed with an *approximation* to $\log Z_\pi$, as would be required in most problems of interest, is no longer guaranteed to show equilibration, but merely *quasi-equilibration*, or equilibration on a portion of the state space. The reason, of course, is that it is always possible that some statistically-vital portion of the state space was missed by the heuristic, resulting in $\log Z_\pi$ being underestimated. Nonetheless, convergence to a linear relation with the correct inverse temperature slope implies that a Boltzmann distribution among states of high probability under the heuristic has been reached.

7 Discussion

We have seen that SSS can yield a powerful query mechanism into an essentially unknown stochastic process that allows construction of an accurate proposal distribution derived from the process. Here, we discuss a few relevant points.

First, we remark that the various aspects of the methodology interact with each other to determine its overall behaviour and performance. An obvious example of such a dependence is between the heuristic algorithm parameters, which, in turn dictate the final distribution, and the SSS tree construction. For SA, of course, the simulation length and annealing schedule predicate the extent to which the ensemble has converged onto the statistically-relevant parts of the target state space. A short SA run will produce a diffuse distribution of high entropy, which may obviously be mismatched to the target. A further consequence, however, is that a relatively large number of calls to the SA process will be required to construct the SSS tree. This is due to the posterior KL loss growing more rapidly during the construction when the distribution being approximated has higher entropy. On the other hand, allowing SA to concentrate onto the relevant parts of the final distribution means that its final entropy is reduced, necessitating fewer calls to the heuristic. This was illustrated clearly in Figure 11; the population for the longest SA run is seen localize to a set of much higher probability than that of shorter runs. Consequently, while each SA run was of course

more demanding, fewer SA calls were required for the longest run. Once again, we emphasize that reliability of the SSS meta-algorithm is ultimately decided by the appropriateness of the heuristic to the distribution of interest.

Other important design parameters, discussed in Appendix 9.2, are the values of the tree construction KL loss threshold θ_0 and the population size N . As one may expect, the population size must generally scale with the problem dimension provided the problem’s entropy does as well. We argue in the Appendix that N must scale linearly with the number of variables to maintain an overall reliability at a fixed level. Though this requirement is parallelisable, and Rao-Blackwellisation can often dramatically mitigate it, albeit in a problem-dependent manner, it is consequently prudent whenever possible to reduce the number of variables under direct simulation by SSS. One possibility to obtain such a reduction is the use of *low-treewidth* methods. The idea is illustrated in Figure 12; displayed is the top layer of a $14 \times 14 \times 14$ Ising lattice. The set of nodes shaded in black, which repeat in each layer of the lattice, represent the variables on which we perform SSS sampling using a heuristic of choice. Once these variables are instantiated, a dynamic programming/transfer matrix algorithm can be used to sample exactly from the blocks of $4 \times 4 \times 14$ variables. The probability of the sample would then simply be that returned by SSS over the black variables multiplied by the exact conditional probability over the remaining variables computed during the block sampling. The number of variables treated by SSS has thus been reduced from the full size (2744 variables) to 728 variables. This technique can be used in conjunction with the parallelisation method discussed in Appendix 9.1 to yield further speedup.

Another observation is that the technique of caching the tree, as described in Section 5, only yields an advantage when the target distribution is highly peaked; in the presence of large randomness, only the root subtree is typically repeatedly visited. The subtrees at lower levels in the tree are overwhelmingly visited once for a reasonable overall number of SSS draws.

Despite the possibilities for reduction in number of variables and the exploitation of parallelism, the conclusion that SSS is quite computationally costly may be unavoidable. However this cost is the price paid for using an analytically-unknown or uncharacterized proposal distribution. A comparison with *population annealing* [25, 33], a state-of-the-art SMC method for the Ising model may yield some perspective. This method approximates expectations by weighted averaging over independent estimators, each derived from a population of *interacting* SA processes. In population annealing, while the SA simulation length must increase with system size to adequately probe the low energy structure of a complex problem, the populations used to compute the estimators can be kept more or less constant. Our algorithm, on the other hand, generally requires linearly scaling the population size and necessitates further recursive calls to the heuristic as the system size increases. In effect, it requires polynomially more work than SMC using annealing. Obviously then, if one were using SA as the heuristic, population annealing is the preferred method. The advantage, of SSS is, of course, is that a more powerful heuristic than SA may be used, which in turn offsets the additional cost. As an extreme, though unrealistic example of this, suppose that one were provided with an oracle that happened to generate, unbeknownst to the user, *perfect* uncorrelated samples from a complex target defined over a large number of variables. In such a scenario, SSS would yield

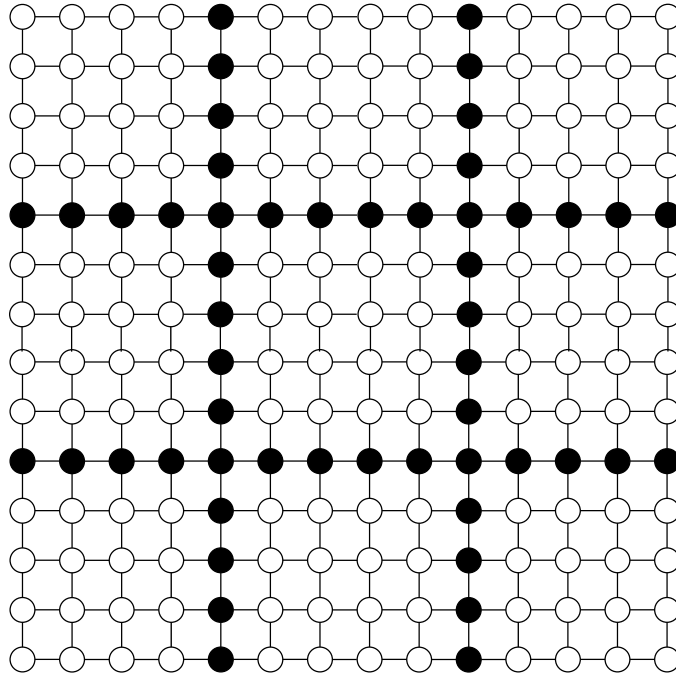


Figure 12: Top view of a $14 \times 14 \times 14$ Ising lattice; the black nodes, repeated in each layer of the lattice, indicate the set of variables on which SSS would perform sampling by using a chosen heuristic. Once these nodes have been fully sampled and instantiated, the remaining blocks of $4 \times 4 \times 14$ variables, filled in white, can be sampled exactly by exploiting their low treewidth. The number of variables under explicit consideration by SSS is thus reduced from $m = 14^3 = 2744$ to $m = 728$ variables, namely, the total number black nodes in the 14 layers. Noting furthermore that once two sections of the system have been broken into disjoint components, simulation within SSS can proceed in parallel, an additional possibility for speedup exists as described in Appendix 9.1.

reliable estimators, including those of the log partition function, using relatively modest resources. SA on the other hand, would give exponentially-degrading performance.

We turn briefly to a discussion of the various heuristics that can conceivably be used with the SSS algorithm. As we have seen, some natural examples that can be employed to compute equilibrium expectations are:

- Stochastic local search methods
- Physically-implemented heuristic algorithms
- Evolutionary/genetic algorithms

However the list can be expanded to include more abstract and mathematically-founded routines. We recall that within the field of combinatoric *optimization*, several algorithms exist that are known to yield good *approximate* solutions [21, 42]. Among these are:

- Linear programming with solution rounding
- Primal-dual algorithms
- Polynomial-time approximation schemes (when they exist)

Furthermore, in some situations such as the *graph matching* problem, computing a minimum solution to a cost function is polynomially feasible [35] but sampling uniformly over *all* such minimizers (or more generally, over low-cost configurations) is highly nontrivial. Usage of one of these methods for the sampling problem is tempting, but several are *deterministic* in their basic forms and so would require a *randomization* strategy to generate a distribution of possible solutions. One obvious such strategy is to randomly perturb the problem parameters prior to each invocation of the heuristic. The resultant states would hence be generated from an analytically unknown proposal distribution, which may serve as a reasonable surrogate to the target distribution at low temperature. As a concrete example, which can easily be seen to be a form of partition function estimation, consider the problem of counting maximum weight matchings (MWM) on a given graph. One may invoke a polynomial time algorithm [13] to compute MWMs of a set of randomized edge weight problems, rejecting all solutions whose costs with respect to the original problem are less than that of the (known) maximum value. A generally nonuniform and unknown distribution over maximum weight matchings to the graph is instantiated; invoking such an algorithm within the SSS framework allows the nonuniformity bias to be corrected for.

Finally, we note that a natural direction of future work, which was not pursued experimentally in this paper, is the analysis of different heuristics within the MCMC context presented in Section 4.2.

We believe that the ideas presented in this paper and the SSS methodology in particular have an appropriate place in the toolbox of practitioners of numerical Monte Carlo simulation. They open the possibility of using arbitrary stochastic heuristics to sample from discrete-valued complex

systems. Of course, SSS should never be used when a better algorithm is known, for example where exact or fast-mixing sampling algorithms exist. As a tool, it should be viewed very much as a “crowbar” with which to pry open the properties of stochastic heuristics. Given this recommendation, and the extensive usage of the concept of recursion in this work, we can think of no better summary of the appropriate attitude to SSS than by recursively paraphrasing A. Sokal’s [40] advice on Monte Carlo strategies in general as follows:

Guideline 1. *State space sampling is an extremely bad Monte Carlo method. It should be used only when all alternative Monte Carlo methods are worse.*

8 Acknowledgements

We acknowledge discussions with and the helpful insights of W. Macready, J. Raymond, H. Katzgraber, P. Carbonetto, M. Amin, and A. Smirnov. F.H. wishes to particularly thank the Vancouver Board of Parks and Recreation for its masterful job in maintaining the beaches under its purview so that work on this project in the Summer of 2015 was a true pleasure.

9 Appendix

9.1 Recursive Partitioning for Sparse Models

In many situations, such as the simulation of two or three dimensional Ising models, the distribution of interest can be interpreted as possessing certain topological properties. We outline a methodology for exploiting the structure of a target distribution to impose a *parallelisability* to the algorithm distinct from the trivial one arising from the population-based aspect of the SCP. The notion of *conditional independence* is key here. Given three sets of variable indices A, B, C , x_A and x_B are said to be conditionally independent given x_C iff

$$\pi(x_A, x_B | x_C) = \pi(x_A | x_C) \pi(x_B | x_C)$$

As an example to illustrate the idea, we consider the case of an Ising model defined on an $L \times L$ grid.

The following discussion is illustrated in Figure 13. Let us initially define the full set of nodes in the grid to be R_{11} and take the set of graph locations $A_{11} \in R_{11}$ to be the set of nodes that vertically bisect (as closely as possible) the grid into two equal-sized rectangular regions. Call the left and right regions R_{12} and R_{22} respectively. We note that in the target distribution,

$$\pi(y_{R_{12}}, y_{R_{22}} | y_{A_{11}}) = \pi(y_{R_{12}} | y_{A_{11}}) \pi(y_{R_{22}} | y_{A_{11}})$$

If, after constraining variables $y_{A_{11}}$ the proposal is then run independently on the two regions, then it will of course, also have this property, i.e.

$$q(u_{R_{12}}, u_{R_{22}} | y_{A_{11}}, \mathbf{x}) = q(u_{R_{12}} | y_{A_{11}}, \mathbf{x}) q(u_{R_{22}} | y_{A_{11}}, \mathbf{x})$$

This suggests that judiciously selecting the variable ordering allows one to *divide and conquer* the problem. In particular, to simulate $\{U_{R_{12}}, U_{R_{22}}\} \sim q(u_{R_{12}} u_{R_{22}} | y_{A_{11}}, \mathbf{x})$, conditional independence allows us to simultaneously generate

$$\begin{aligned} \{U_{R_{12}}\} &\sim q(u_{R_{12}} | y_{A_{11}}, \mathbf{x}) \\ \{U_{R_{22}}\} &\sim q(u_{R_{22}} | y_{A_{11}}, \mathbf{x}) \end{aligned}$$

as well as variables $Y_{R_{12}}, Y_{R_{22}}$ using parallel worker threads. As always, the reduction in number of free variables allows one to use fewer resources to simulate the consecutive distributions.

The idea can be applied recursively: suppose in turn that A_{12} is a set of nodes that *horizontally* bisects R_{12} into regions R_{13}, R_{23} respectively, and that A_{22} horizontally bisects R_{22} into regions R_{33}, R_{43} , and we now have *four* conditionally independent sets of variables. The second index in the subscript can be seen to refer to a “level” in a hierarchy, with the first being an identifier at the level. In general, if $A_{i,l}$ are a set of nodes that horizontally bisect grid region $R_{i,l}$ into $\{R_{j,l+1}, R_{k,l+1}\}$ then $A_{j,l+1}, A_{k,l+1}$ will be vertical bisectors of those regions, and vice versa. Let us examine the complexity of the naïve, one-at-a-time SCP algorithm on the $L \times L$ lattice. Initially, the L variables in A_{11} are assigned sequentially. Once $Y_{A_{11}}$ have been assigned, exploiting conditional independence effectively allows us to process sets A_{12}, A_{22} , in $O(L/2)$ instead of $O(L)$ time. Clearly, in the next step we can sample from four bisecting sets in effective $O(L/4)$ time, and so on. Hence, by exploiting the inherent parallelism emerging from the problem structure and variable ordering, the complexity of the one-at-a-time SCP algorithm is effectively reduced from $O(L^2)$ to $O(L \log L)$.

For graphs of general topology, the task of finding a set of variables that maximize the inherent parallelism of the sampling problem is known as the *vertex separator problem (VSP)*. In general, VSP is an NP-hard problem [6], but there exist several useful heuristics [11] that may give a satisfactory variable ordering.

9.2 Selecting the parameters for SSS

Recall from the SSS algorithm description that we set a KL loss threshold θ_0 and grow the state space tree representation until this threshold is violated, recursively calling the heuristic to continue growing the tree as needed. One may naturally wonder how to set θ_0 and the population size N to ensure a given accuracy at any system size. After all, if θ_0 and N are held constant while larger systems are simulated, the overall divergence between the estimate and the true distribution will increase. In this section, we argue that N should be allowed to increase linearly with system size, though we remind the reader that this is a highly parallelisable burden.

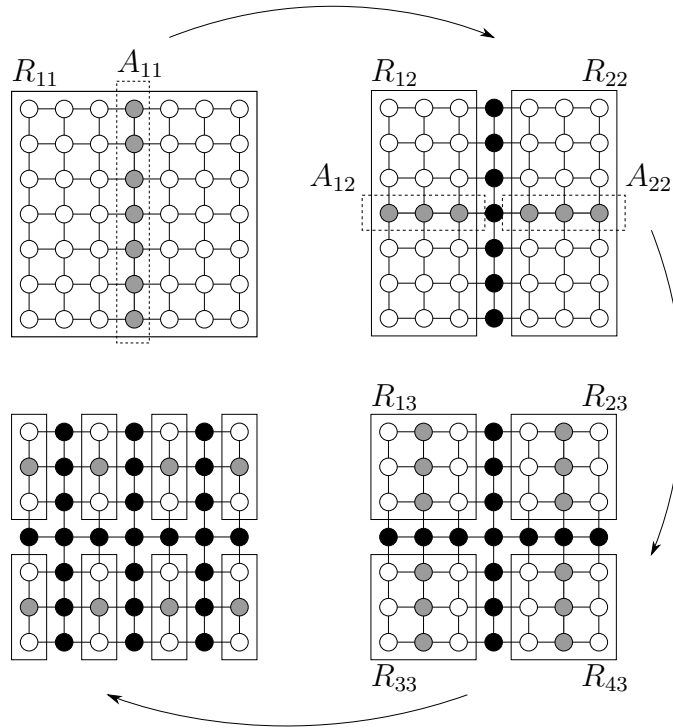


Figure 13: Exploiting conditional independence to accelerate sampling on a 7×7 grid. Initially, samples are sequentially drawn from the vertical shaded column in the top left, called A_{11} . The two sets of variables separated by the column are R_{12}, R_{22} . Once the variables in A_{11} are sampled, the variables in R_{12}, R_{22} are independent. In the top right, sampling within these regions proceeds simultaneously along A_{12}, A_{22} , the horizontal bisectors of the regions. The bisection-based ordering introduces an accelerating “parallelism” in that as the graph becomes increasingly partitioned, an increasing number variables can be sampled simultaneously. The effective complexity of the sampling process is reduced from $O(L^2)$ to $O(L \log L)$, where L is the length of the grid.

Suppose we observe in an m -variable system that SSS typically requires around N_{calls} calls to the heuristic process to generating a sample. The value of N_{calls} depends on the target distribution entropy, with larger entropy necessitating larger N_{calls} . Under KL loss threshold θ_0 , the *overall* KL divergence between the target and the estimator will be $\sim N_{calls}\theta_0$. Suppose for simplicity that the target is uniform. Then doubling the system size m will consequently double the required N_{calls} and hence the total divergence. If, however, we *halved* the partition construction tolerance for the larger system to $\theta_0/2$ and *doubled* the population size N , then N_{calls} will still double over that of the m -variable system. This is because the sizes of the constructed subtrees under parameters $\theta_0/2$ and $2N$ will be approximately the same as under θ_0 and N , which in turn follows from the fact that the posterior KL loss essentially becomes $O(1/N)$ for moderate-to-large N . The effect is therefore that the *total* divergence reverts to $\sim N_{calls}\theta_0$.

The message is that in general, scaling a system size by a factor of c within a problem class where the entropy increases linearly with size requires reduction and increase of θ_0 and N by a factor of c respectively in order to maintain the KL divergence at a fixed value. Rao-Blackwellisation as described in Section 3.3.3 can often dramatically reduce this number in practice but the discussion in this section at least provides a conservative general guideline. Experimentation on the problem class may be required to select an efficient population size.

9.3 Bayesian Updating of State Space Trees

As mentioned in the text, one of the advantages of Bayesian estimators is their natural ability to adapt to more data that may arrive. In this section, we consider informally how to implement this functionality within the SSS methodology. Doing so is not onerous but does require a certain amount of bookkeeping and care, especially when combined with memory-bounding.

It is more appropriate in the present context to consider the full state space tree as a collection of *concatenated* subtrees corresponding to state space partitions, each endowed with probability estimates over its nodes. When the root node of such a subtree, receives a certain number of visits, further runs to the SCP with the appropriate condition are made, but only the probability estimates corresponding to nodes of the *original* partition are updated. Nodes belonging to downstream subtrees require their own refresh. When retracting a subleaf node, the Dirichlet aggregation property implies that the prior parameter of the new leaf node is simply the sum of its two deleted childrens'. Hence, Bayes estimators on pruned trees resulting from retraction can be updated without issue.

One complication with Bayesian updating in the presence of retraction is that in principle, once probability estimates in a subtree are modified, the probabilities of *all* nodes descended from this tree are changed as well. This implies that the subleaf probability values comprising the deletion priority in the retraction queue will no longer correspond to their actual probabilities. Updating these values can become quite expensive, so a natural option is to simply use the “stale” initially-computed probabilities as deletion priorities. This does not affect the correctness of the algorithm; subleaf nodes could even have been dropped at random. The idea behind the prioritization is

to simply avoid removing representations that are likely to be used multiple times. The initial approximations are likely accurate enough to effect this behaviour satisfactorily.

References

- [1] M. Abramowitz and I. A. Stegun. *Handbook of mathematical functions: with formulas, graphs, and mathematical tables*. Courier Corporation, 1964.
- [2] J. Berger. The robust bayesian viewpoint (with discussion). *Robustness of Bayesian Analysis*, pages 63–124, 1984.
- [3] J. O. Berger. *Statistical decision theory and Bayesian analysis*. Springer Science & Business Media, 2013.
- [4] J. M. Bernardo and A. F. Smith. *Bayesian theory*, volume 405. John Wiley & Sons, 2009.
- [5] K. Binder and A. P. Young. Spin glasses: Experimental facts, theoretical concepts, and open questions. *Reviews of Modern physics*, 58(4):801, 1986.
- [6] T. N. Bui and C. Jones. Finding good approximate vertex and edge partitions is np-hard. *Information Processing Letters*, 42(3):153–159, 1992.
- [7] G. Casella and C. Robert. Rao-blackwellisation of sampling schemes. *Biometrika*, 81(1):81–94, 1996.
- [8] D. Chandler. Introduction to modern statistical mechanics. *Introduction to Modern Statistical Mechanics, by David Chandler, pp. 288. Foreword by David Chandler. Oxford University Press, Sep 1987. ISBN-10: 0195042778. ISBN-13: 9780195042771*, 1, 1987.
- [9] T. H. Cormen. *Introduction to algorithms*. MIT press, 2009.
- [10] C. P. De Campos and A. Benavoli. Inference with multinomial data: why to weaken the prior strength. In *IJCAI Proceedings-International Joint Conference on Artificial Intelligence*, volume 22, page 2107, 2011.
- [11] C. de Souza and E. Balas. The vertex separator problem: algorithms and computations. *Mathematical Programming*, 103(3):609–631, 2005.
- [12] P. Del Moral, A. Doucet, and A. Jasra. Sequential monte carlo samplers. *Journal of the Royal Statistical Society: Series B (Statistical Methodology)*, 68(3):411–436, 2006.
- [13] J. Edmonds. Paths, trees, and flowers. *Canadian Journal of mathematics*, 17(3):449–467, 1965.

- [14] S. Geman and D. Geman. Stochastic relaxation, gibbs distributions, and the bayesian restoration of images. *Pattern Analysis and Machine Intelligence, IEEE Transactions on*, (6):721–741, 1984.
- [15] C. Geyer. Computing science and statistics: Proceedings of the 23rd symposium on the interface. *American Statistical Association, New York*, page 156, 1991.
- [16] R. J. Glauber. Time-dependent statistics of the ising model. *Journal of mathematical physics*, 4(2):294–307, 1963.
- [17] D. E. Goldberg. *Genetic algorithms*. Pearson Education India, 2006.
- [18] I. J. Good. *The estimation of probabilities: An essay on modern Bayesian methods*. M.I.T. Press, 1965.
- [19] F. Hamze. Robust bayesian multinomial inference via posterior plausibility. *In preparation*, 2015.
- [20] W. K. Hastings. Monte carlo sampling methods using markov chains and their applications. *Biometrika*, 57(1):97–109, 1970.
- [21] D. S. Hochbaum. *Approximation algorithms for NP-hard problems*. PWS Publishing Co., 1996.
- [22] J. H. Holland. *Adaptation in natural and artificial systems: an introductory analysis with applications to biology, control, and artificial intelligence*. MIT press, 1992.
- [23] H. H. Hoos and T. Stützle. *Stochastic local search: Foundations & applications*. Elsevier, 2004.
- [24] J. Houdayer. A cluster monte carlo algorithm for 2-dimensional spin glasses. *The European Physical Journal B-Condensed Matter and Complex Systems*, 22(4):479–484, 2001.
- [25] K. Hukushima and Y. Iba. Population annealing and its application to a spin glass. In *The Monte Carlo Method in the Physical Sciences: Celebrating the 50th Anniversary of the Metropolis Algorithm*, volume 690, pages 200–206. AIP Publishing, 2003.
- [26] K. Hukushima and K. Nemoto. Exchange monte carlo method and application to spin glass simulations. *Journal of the Physical Society of Japan*, 65(6):1604–1608, 1996.
- [27] C. Jarzynski. Nonequilibrium equality for free energy differences. *Physical Review Letters*, 78(14):2690, 1997.
- [28] M. Jerrum and A. Sinclair. The markov chain monte carlo method: an approach to approximate counting and integration.

- [29] M. Johnson, M. Amin, S. Gildert, T. Lanting, F. Hamze, N. Dickson, R. Harris, A. Berkley, J. Johansson, P. Bunyk, et al. Quantum annealing with manufactured spins. *Nature*, 473(7346):194–198, 2011.
- [30] T. Kadowaki and H. Nishimori. Quantum annealing in the transverse ising model. *Physical Review E*, 58(5):5355, 1998.
- [31] H. G. Katzgraber, M. Körner, and A. Young. Universality in three-dimensional ising spin glasses: A monte carlo study. *Physical Review B*, 73(22):224432, 2006.
- [32] T. Li. Structure of metastable states in a random ising chain. *Physical Review B*, 24(11):6579, 1981.
- [33] J. Machta. Population annealing with weighted averages: A monte carlo method for rough free-energy landscapes. *Physical Review E*, 82(2):026704, 2010.
- [34] N. Metropolis, A. W. Rosenbluth, M. N. Rosenbluth, A. H. Teller, and E. Teller. Equation of state calculations by fast computing machines. *The journal of chemical physics*, 21(6):1087–1092, 1953.
- [35] C. H. Papadimitriou and K. Steiglitz. *Combinatorial optimization: algorithms and complexity*. Courier Corporation, 1998.
- [36] W. Perks. Some observations on inverse probability including a new indifference rule. *Journal of the Institute of Actuaries*, pages 285–334, 1947.
- [37] S. Russell. Efficient memory-bounded search methods. *ECAI-1992, Vienna, Austria*, 1992.
- [38] S. Russell and P. Norvig. *Artificial intelligence: a modern approach*. 1995.
- [39] T. Sejnowski. Learning and relearning in boltzmann machines. *Graphical Models: Foundations of Neural Computation*, page 45, 2001.
- [40] A. Sokal. *Monte Carlo methods in statistical mechanics: foundations and new algorithms*. Springer, 1997.
- [41] R. H. Swendsen and J.-S. Wang. Nonuniversal critical dynamics in monte carlo simulations. *Physical review letters*, 58(2):86, 1987.
- [42] V. V. Vazirani. *Approximation algorithms*. Springer Science & Business Media, 2013.
- [43] W. Wang, J. Machta, and H. G. Katzgraber. Population annealing: Theory and application in spin glasses. *arXiv preprint arXiv:1508.05647*, 2015.

- [44] U. Wolff. Collective monte carlo updating for spin systems. *Physical Review Letters*, 62(4):361, 1989.
- [45] W. Zhang. *State-space search: Algorithms, complexity, extensions, and applications*. Springer Science & Business Media, 1999.
- [46] Z. Zhu, A. J. Ochoa, and H. G. Katzgraber. Efficient cluster algorithm for spin glasses in any space dimension. *arXiv preprint arXiv:1501.05630*, 2015.
- [47] Z. Zhu, A. J. Ochoa, S. Schnabel, F. Hamze, and H. G. Katzgraber. Best-case performance of quantum annealers on native spin-glass benchmarks: How chaos can affect success probabilities. *arXiv preprint arXiv:1505.02278*, 2015.